

Rare Top-quark Decays to Higgs boson in MSSM

A. DEDES^{1,2*}, M. PARASKEVAS^{1†}, J. ROSIEK^{3‡}, K. SUXHO^{1§}, K. TAMVAKIS^{1¶}

¹*Department of Physics, Division of Theoretical Physics,
University of Ioannina, GR 45110, Greece*

²*University of Athens, Physics Department,
Nuclear and Particle Physics Section, GR 15771 Athens, Greece*

³*Institute of Theoretical Physics, Warsaw University,
Hoza 69, 00-681 Warsaw, Poland*

January 1, 2023

Abstract

In full one-loop generality and in next-to-leading order in QCD, we study rare top to Higgs boson flavour changing decay processes $t \rightarrow q h$ with $q = u, c$ quarks, in the general MSSM with R-parity conservation. Our primary goal is to search for enhanced effects on $\mathcal{B}(t \rightarrow q h)$ that could be visible at current and high luminosity LHC running. To this end, we perform an analytical expansion of the amplitude in terms of flavour changing squark mass insertions that treats both cases of hierarchical and degenerate squark masses in a unified way. We identify two enhanced effects allowed by various constraints: one from holomorphic trilinear soft SUSY breaking terms and/or right handed up squark mass insertions and another from non-holomorphic trilinear soft SUSY breaking terms and light Higgs boson masses. Interestingly, even with $\mathcal{O}(1)$ flavour violating effects in the, presently unconstrained, up-squark sector, SUSY effects on $\mathcal{B}(t \rightarrow q h)$ come out to be unobservable at LHC mainly due to leading order cancellations between penguin and self energy diagrams and the constraints from charge- and colour-breaking minima (CCB) of the MSSM vacuum. An exception to this conclusion may be effects arising from non-holomorphic soft SUSY breaking terms in the region where the CP-odd Higgs mass is smaller than the top-quark mass but this scenario is disfavoured by recent LHC searches. Our calculations for $t \rightarrow q h$ decay are made available in `SUSY_FLAVOUR` numerical library.

*email: adedes@cc.uoi.gr

†email: mparask@grads.uoi.gr

‡email: janusz.rosiek@fuw.edu.pl

§email: csoutzio@cc.uoi.gr

¶email: tamvakis@uoi.gr

1 Introduction

The last fundamental elementary particles discovered during the last 20 years are the tau-neutrino by DONUT Collaboration [1], the top quark at Tevatron [2,3] with mass $m_t = 172.5$ GeV and the Higgs boson [4–6] at LHC [7,8], with mass $m_h \approx 126$ GeV. Among them, the top quark has been and will be produced in large numbers at LHC, allowing for increasingly accurate measurements of its properties. LHC operating at c.m. energy of 7 and 8 TeV has already collected about two-million $t\bar{t}$ -pairs. It is therefore timely to examine the possibility of rare, flavour-changing (FC), top decays to the light up-quarks, u or c , and the Higgs boson h ,

$$t \rightarrow u h, \quad \text{or} \quad t \rightarrow c h. \quad (1.1)$$

We collectively denote these processes as $t \rightarrow q h$ with $q = u, c$. The Higgs boson field h is understood as one of the possible scalar fields that couples to up-quarks and has mass smaller than that of the top-quark.

If the decays $t \rightarrow q h$ are governed only by the Standard Model (SM) [9] dynamics they would never be observed at LHC because their branching ratios, $\mathcal{B}(t \rightarrow u h)_{\text{SM}} \approx 4 \times 10^{-17}$ and $\mathcal{B}(t \rightarrow c h)_{\text{SM}} \approx 4 \times 10^{-14}$ [10, 11], are tiny. This extraordinary suppression is caused because, firstly, the Glashow-Iliopoulos-Maiani (GIM) [12] suppression prohibits the loop diagram leading contribution for $t \rightarrow q h$, and secondly, because the quarks circulating in the $t \rightarrow q h$ loop amplitude are those of down type with small mass differences.

On the contrary, in a well motivated extension of the SM, the R-parity conserving Minimal Supersymmetric Standard Model (MSSM) [13–15], although the GIM mechanism is still operative in the quark-interactions, it is not, in general, in the squark interactions. Eventually, coloured scalars, the squarks, enter in loops with potentially large mass differences. The question is then whether these new interactions are able to enhance $\mathcal{B}(t \rightarrow q h)$ up to an observable level at LHC. Depending on MSSM input parameters, Guasch and Sola [16] arrived at a maximum prediction $\mathcal{B}(t \rightarrow c h) \approx 4 \times 10^{-4}$, while a more recent analysis by Cao *et.al* [17, 18], taking into account constraints from rare B -meson decays, concluded a maximum branching fraction of up to $\mathcal{B}(t \rightarrow c h) \approx 6 \times 10^{-5}$ (for an earlier study see also ref. [19]). Finally, not long ago, a new analysis by the authors of ref. [20] concluded a maximum branching ratio at the level of $O(10^{-6})$ after constraints.

The relevant Lagrangian governing the rare top decays $t \rightarrow q h$ in the physical quark basis, after integrating out all heavy degrees of freedom, is simply,

$$-\mathcal{L} \supset C_L^{(h)} \bar{q}_R t_L h + C_R^{(h)} \bar{q}_L t_R h + \text{H.c.}, \quad (1.2)$$

with dimensionless (Wilson) coefficients $C_{L,R}^{(h)}$. Note that in the MSSM h may stand for one of the two CP-even Higgs bosons denoted as h, H , respectively. Currently LHC sets an upper bound [21, 22]

$$\mathcal{B}(t \rightarrow q h) \leq 0.79\% \quad (\text{ATLAS}), \quad \mathcal{B}(t \rightarrow q h) \leq 0.56\% \quad (\text{CMS}). \quad (1.3)$$

This result places rather weak restrictions onto the Wilson coefficients: $|C_L|, |C_R| \lesssim 0.1$. In renormalisable theories like the MSSM, the coefficients C_L and C_R would come from one-loop diagrams involving gluino (or neutralino)-up squarks, chargino-down squarks and charged Higgs-down quarks. The gluino-loop gives the dominant contribution to $\mathcal{B}(t \rightarrow q h)$ that generically is of the order $\alpha_s/4\pi \approx 0.01$, which is by an order of magnitude less than

the current bound, but probably within LHC's projected reach at $\sqrt{s} = 14$ TeV with 3000 fb $^{-1}$ [23] (see also note [24])

$$\mathcal{B}(t \rightarrow q h) \lesssim 2.0 \times 10^{-4} \Leftrightarrow |C_L|, |C_R| \lesssim \mathcal{O}(1) \times 10^{-2}. \quad (1.4)$$

There are already many phenomenological studies for these decays, a partial list included in [25–31]. Very recently in [32, 33], plausible techniques that distinguish between $t \rightarrow u h$ and $t \rightarrow c h$ have been suggested. It is therefore worth looking for MSSM branching fraction predictions from both rare top decays, $t \rightarrow u h$ and $t \rightarrow c h$.

The new flavour structure in the MSSM Lagrangian can be parametrized in terms of supersymmetry soft breaking squark mass matrices $m_{Q_L}, m_{U_R}, m_{D_R}$ and trilinear holomorphic A_U, A_D matrices as well as the trilinear non-holomorphic A'_U, A'_D matrices [34–37]¹

$$\begin{aligned} \mathcal{L}_{\text{MSSM}} \supset & -\tilde{Q}_L^\dagger m_{Q_L}^2 \tilde{Q}_L - \tilde{U}_R^\dagger m_{U_R}^2 \tilde{U}_R - \tilde{D}_R^\dagger m_{D_R}^2 \tilde{D}_R \\ & + \left(H_2 \tilde{Q}_L A_U \tilde{U}_R + H_1 \tilde{Q}_L A_D \tilde{D}_R + \text{H.c.} \right) \\ & + \left(H_1^\dagger \tilde{Q}_L A'_U \tilde{U}_R + H_2^\dagger \tilde{Q}_L A'_D \tilde{D}_R + \text{H.c.} \right), \end{aligned} \quad (1.5)$$

where flavour and gauge group indices have been suppressed. As we already mentioned, soft breaking terms in (1.5) may have non-trivial structure, so that the quark and squark mass matrices cannot be diagonalized simultaneously in the same flavour basis. However, a fully generic structure for these matrices is far excluded by Kaon, charm, and B -physics experiments with the *exception* of the right handed up-squark mass matrix $m_{U_R}^2$ and the trilinear soft SUSY breaking matrices A_U and A'_U . For all other matrices m and A in (1.5), “flavour” experiments help to single out four possible categories:

1. Minimal Flavour Violation (MFV) assumption [35, 38]: flavour violation arises only from Yukawa matrices Y_U and Y_D .
2. Almost degenerate m 's - their diagonal elements proportional to the unit matrix; A 's almost diagonal; small off-diagonal terms in m 's and A 's.
3. As in point (2) but m 's become hierarchical: 1st and 2nd generation are much heavier than the third. In this case off-diagonal squark mass matrix elements may be of order one.
4. Alignment: no particular hierarchy among diagonal squark masses, but small squark mixing angles, enforced by some symmetries, as required by experimental constraints.

MFV basically leads to the same suppression pattern for $t \rightarrow q h$ as in the SM and therefore no signal observation is expected at LHC [39]². We need therefore to depart from MFV.

¹Non-holomorphic terms may arise from the Kähler potential non-renormalizable operators like for example $XX^\dagger H_1^\dagger Q_L U_R / M^3$ interaction between MSSM superfields and hidden sector superfield X whose F-term vev, $\langle F_X \rangle$, is responsible for spontaneous SUSY breaking in the hidden sector. In contrast, the holomorphic SUSY breaking terms arise from superpotential non-renormalizable operators like, $X H_2 Q_L U_R / M$. If SUSY breaking mediators of mass $\mathcal{O}(M)$ are very heavy, as for instance in gravity mediated SUSY breaking scenario where $M = M_{Pl}$, then non-holomorphic terms (A'_U) are negligible compared to the holomorphic ones (A_U). However, they could both be of the same order of magnitude if SUSY breaking happens at low SUSY breaking scales, comparable to electroweak scale [36].

²This is also due to the fact that no $\tan \beta$ enhanced top flavour changing decay amplitudes arise in the MSSM as we will see shortly.

This is most conveniently done by considering the dimensionless flavour violating expansion parameters (commonly called “mass insertions”) [40, 41]:

$$\Delta_{\tilde{X}}^{IJ} = \frac{(m_X^2)^{IJ}}{\sqrt{(m_X^2)^{II} (m_X^2)^{JJ}}}, \quad (1.6)$$

which denotes the ratio of flavour-violating squark mass matrix elements over an average of flavour-conserving squark mass matrix elements (\tilde{X} can be \tilde{U} or \tilde{D}). It has been shown in ref. [42] that, for $\Delta F = 1$ processes, the same (in magnitude) Δ -parameter can be used to parametrize flavour effects in both cases of hierarchical and degenerate squark masses, although the Δ -parameter may have different meaning in each case. We develop a similar technique here in expanding the full amplitude for $t \rightarrow q h$ in powers of Δ ’s and therefore discussing cases (2) and (3) in a unified way.

In the fourth case of alignment quark and squark mass matrices are forced by some approximate flavour symmetry to be diagonalized almost by the same field rotation. This means that the remaining squark rotation angles in the super-CKM basis are small, but in general, squark masses are far from degenerate leading to serious constraints from K-physics. In any case, having the light Higgs boson mass at 126 GeV, one needs pushing the stop mixing angle to the maximal value. This situation does not fit naturally to the case of small mixing angles. On this ground we will not examine this case.

In fact we shall show below that the LHC projected bound (1.4) is impossible to be reached in the general R-parity conserved MSSM with degenerate or hierarchical squark mass spectrum. This is partly due to cancellations between self energy and penguin contributions prohibiting non-decoupling SUSY effects. As a result, in the best case scenario, and before constraints, an estimate of the dominant gluino-squark diagrams results in

$$C_{L,R}^{(h)} \approx \frac{\alpha_s}{4\pi} \left(\frac{m_t}{M_S} \right)^2 \Delta \lesssim 2 \times 10^{-4}, \quad (1.7)$$

for degenerate SUSY squark masses M_S at 1 TeV scale and $\Delta = \mathcal{O}(1)$. Similar cancellations exist in the chargino-squark loops but now $\alpha_s \rightarrow \alpha_2$ and therefore, following (1.7), $C_{L,R}^{(h)}$ are by at least a factor of three smaller than the gluino contribution.³ Furthermore, as it is obvious from (1.7), and contrary to recent claims in the literature [20], both our analytical and numerical study concludes that there are *no* non-decoupling effects whatsoever for large SUSY mass spectrum, collectively indicated here as M_S .

To the best of our knowledge, this study deals with four new aspects of $\mathcal{B}(t \rightarrow q h)$ not considered before in the literature:

1. We take into account the effects of Next to Leading order QCD corrections due to the SUSY loop induced chromomagnetic dipole operator and the running of operators from the SUSY scale M_S to the top quark scale (see Section 2).
2. We present analytical details of the cancellations and decoupling (Section 3), using a common scheme for both universal and hierarchical squark mass structures.

³In fact chargino diagrams are far smaller than that because of the down squark circulation in loop. The relevant $\Delta_{\tilde{D}}$ ’s in this case must be small to respect experimental constraints from low energy meson experiments. Similar situation applies to charged Higgs boson one-loop diagrams.

3. We investigate the effect on $\mathcal{B}(t \rightarrow q h)$ from non-holomorphic SUSY breaking terms A'_U [see eq. (1.5)] (Section 5).
4. Finally, we have encoded all our calculations into a publicly available⁴ `SUSY_FLAVOUR` library [43–45]. `SUSY_FLAVOUR` uses the relevant and most complete up-to-date constraints from FCNC processes (Section 4).

2 Calculation of $\mathcal{B}(t \rightarrow q h)$ in MSSM

The gauge-invariant dimension-6 operator responsible for the decay $t \rightarrow q h$ can be, after decoupling of heavy particles, simply written as⁵

$$O^{(h)} = \left(H^\dagger H \right) \bar{Q}_L^I u_R^J \tilde{H} + \text{H.c.} \quad (2.1)$$

H is the SM Higgs field $SU(2)$ doublet, $\tilde{H} = i\sigma_2 H^*$ is its charged conjugate, indices I and J denote quark flavours, Q_L^I is the left-handed quark $SU(2)$ doublet while u_R^J is the right-handed up-quark singlet. $SU(2)$ and $SU(3)$ indices are not shown explicitly. The effective operator in $O^{(h)}$ is of (pseudo)-scalar form and affects the renormalizable Yukawa interaction $\bar{Q}_L^I u_R^J \tilde{H}$. After electroweak symmetry breaking (EWSB) it results in the effective Lagrangian (1.2).

It was shown recently in ref. [46] that the operator $O^{(h)}$ mixes through QCD strong interactions with the gluonic dipole operator that has the form

$$O^{(g)} = g_s \bar{Q}_L^I \sigma^{\mu\nu} \lambda^A u_R^J \tilde{H} G_{\mu\nu}^A + \text{H.c.}, \quad (2.2)$$

where $g_s = \sqrt{4\pi\alpha_s}$ is the strong QCD coupling, λ^A are the Gell-Mann matrices, while $G_{\mu\nu}^A$ is the $SU(3)$ field strength tensor. Like the operator $O^{(h)}$, the operator $O^{(g)}$ is also chirality flipping. After EWSB it results in the effective Lagrangian term

$$-\mathcal{L} \supset C_L^{(g)IJ} \bar{u}_R^I \sigma_{\mu\nu} \lambda^A u_L^J G^{A\mu\nu} + C_R^{(g)IJ} \bar{u}_L^I \sigma_{\mu\nu} \lambda^A u_R^J G^{A\mu\nu} + \text{H.c.} \quad (2.3)$$

Having listed all operators needed, we enumerate here our steps in calculating $\mathcal{B}(t \rightarrow q h)$:

1. Full calculation of the relevant 1-Particle-Irreducible (1PI) Feynman diagrams $C_{L,R}^{(h)}$ at scale M_S , where M_S is the lightest coloured sparticle (squark or gluino) mass.
2. Full calculation of the SUSY induced Wilson coefficient $C_{L,R}^{(g)}$ associated with the dipole operator $O^{(g)}$ that mix with strong (QCD) quantum corrections.
3. Use Renormalization Group Equations (RGEs) with formulae taken from [46] to run all operators down to the top mass scale.
4. Calculate the branching fraction at m_t^{pole} .

In the next two subsections we append technical details entailed in these steps.

⁴`SUSY_FLAVOUR` can be downloaded from http://www.fuw.edu.pl/susy_flavor

⁵In full SUSY limit with all Higgs (super)fields present, the corresponding operator is an F-term and, therefore, holomorphic. It has the form $O^{(h)} = (H_1 H_2) Q_L^I u_R^J H_2 + \text{H.c.}$. Note that this operator breaks Peccei-Quin and R-symmetry invariance and therefore its Wilson coefficient must be proportional to quantities that violate these symmetries, such as the gluino mass, the trilinear soft SUSY breaking couplings and the μ -parameter, *c.f.* eq. (3.9).

2.1 Branching ratio and QCD corrections

In this Section we present the calculation for the decay of the top quark into a light quark $q = u, c$ and a CP-even Higgs boson $h \equiv (H \text{ or } h)$ including NLO QCD corrections. In the limit $m_q \approx 0$ the tree level decay rate reads:⁶

$$\Gamma_0(t \rightarrow q h) = \frac{m_t}{32\pi} \left(|C_L^{(h)}|^2 + |C_R^{(h)}|^2 \right) \left(1 - \frac{m_h^2}{m_t^2} \right)^2, \quad (2.4)$$

with $C_{L,R}^{(h)}$ defined in eq. (1.2). At the top-quark mass scale, $\mu = m_t$, the following QCD NLO decay rate is found [46],

$$\begin{aligned} \Gamma(t \rightarrow q h) &= 1.018 \Gamma_0 \\ &+ 0.049 \frac{m_t^3}{16\pi v} \left(1 - \frac{m_h^2}{m_t^2} \right)^2 \Re \left[C_R^{(h)*} C_R^{(g)} + C_L^{(h)*} C_L^{(g)} \right], \end{aligned} \quad (2.5)$$

with $C_{L,R}^{(g)}$ defined in eq. (2.3). We use $\alpha_s(m_t) = 0.1079$, $m_t(m_t)_{\overline{DR}} = 163.6$ GeV, $m_t^{pole} = 172.5$ GeV, $G_F = 1/\sqrt{2}v^2 = 1.1664 \times 10^{-5}$ GeV⁻². In our results we have neglected terms proportional to $|C_{L,R}^{(g)}|^2$ since they are small for $m_h \simeq 126$ GeV. For the branching fraction $\mathcal{B}(t \rightarrow q h)$, the next-to-next-to-leading order top quark width is used, $\Gamma(t \rightarrow bW) = 1.39$ GeV [47]. Furthermore, we assume that the “tree level” decay width $\Gamma(t \rightarrow bW)$ is not affected substantially by SUSY loop contributions. In this Section, we calculate the Wilson coefficients, $C_{L,R}^{(h)}$ and $C_{L,R}^{(g)}$, at the scale $\mu = M_S = m_{\tilde{g}}$, and use the renormalization group equations [46] to run them down to the scale $\mu = m_t$,

$$\begin{aligned} C_{L,R}^{(h)}(m_t) &= C_{L,R}^{(h)}(M_S) \left(\frac{\alpha_s(M_S)}{\alpha_s(m_t)} \right)^{-4/b_3} \\ &+ \frac{24}{7} \frac{m_t(m_t)^2}{v} C_{L,R}^{(g)}(M_S) \left[\left(\frac{\alpha_s(M_S)}{\alpha_s(m_t)} \right)^{2/(3b_3)} - \left(\frac{\alpha_s(M_S)}{\alpha_s(m_t)} \right)^{-4/b_3} \right], \end{aligned} \quad (2.6a)$$

$$C_{L,R}^{(g)}(m_t) = C_{L,R}^{(g)}(M_S) \left(\frac{\alpha_s(M_S)}{\alpha_s(m_t)} \right)^{2/(3b_3)}, \quad (2.6b)$$

where $b_3 = 11 - 2N_f/3$ is the 1-loop gluon β -function. In our case $N_f = 6$, i.e., we assume there are no other coloured particles below M_S except from the six SM quark flavours. Diagrams that do not involve coloured particles are “frozen” at the m_t -scale and do not participate in the running of Wilson coefficients in eq. (2.6b).

It turns out that the effect of consistently including NLO QCD corrections in $\mathcal{B}(t \rightarrow q h)$ is about 20%. This is primarily due to the RGE running of $C_{L,R}^{(h)}$ from M_S down to the top quark mass scale, and, secondarily due to finite SUSY corrections in $C^{(g)}$ present in the decay width (2.5). The $C^{(h)}$ and $C^{(g)}$ coefficients, although in theory different in their Dirac and Lorentz structures, are both subject to the same squark-gluino Feynman diagram contribution. $C^{(g)}$ has analogous, and even more persisting, cancellations than $C^{(h)}$, due

⁶Although straightforward, decays $t \rightarrow q A$ with A being the CP-odd Higgs boson are only marginally permitted by recent LHC data and therefore not considered in this work, *c.f.*, discussion in Section 5.2.

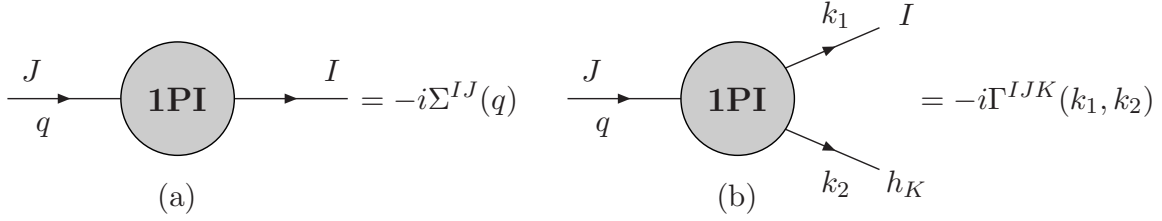


Figure 1: (a) Quark self energy one-particle irreducible (1PI) diagram corrections. (b) 1PI penguin contribution to $u^J \rightarrow u^I + h_K$.

to the flavour conserving gluon-squark vertex of the former, and the same flavour changing insertions i.e., same Δ 's. As a result, it turns out that SUSY contributions to $m_t C^{(g)}$ are at most of the same order as in $C^{(h)}$ and give an amount of 2-10% correction to the decay width.

2.2 Wilson coefficients : full MSSM corrections

Expressions for C -coefficients are more transparent if we write them in terms of the one particle irreducible (1PI) diagrams for self energies (Σ) and penguins (ΔF), as in Fig. 1. We define:

$$\Sigma^{IJ}(p) = \Sigma_{VL}^{IJ}(p^2) \not{p} P_L + \Sigma_{VR}^{IJ}(p^2) \not{p} P_R + \Sigma_{mL}^{IJ}(p^2) P_L + \Sigma_{mR}^{IJ}(p^2) P_R, \quad (2.7)$$

$$\Gamma^{IJK}(k_1, k_2) = \Delta F_L^{IJK}(k_1, k_2) P_L + \Delta F_R^{IJK}(k_1, k_2) P_R. \quad (2.8)$$

All Σ 's and ΔF 's depend on external momenta and internal masses. We follow everywhere the Feynman rules, notation and conventions, from refs. [48, 49]. For specific processes, the top-quark is identified with $J = 3$ and the charm-(up-)quark with $I = 2$ ($I = 1$), the “little h ” Higgs boson with $K = 2$, the “big H ” with $K = 1$, but otherwise we keep the I, J and K notation as general as possible.

Using standard on-shell renormalization scheme techniques we obtain for $I \neq J$:

$$\begin{aligned} C_L^{(h) IJK} &= \frac{\eta^K}{m_J^2 - m_I^2} \left\{ m_I m_J^2 \left[\Sigma_{VL}^{IJ}(m_J^2) - \Sigma_{VL}^{IJ}(m_I^2) \right] + m_I^2 m_J \left[\Sigma_{VR}^{IJ}(m_J^2) - \Sigma_{VR}^{IJ}(m_I^2) \right] \right. \\ &+ m_I m_J \left[\Sigma_{mR}^{IJ}(m_J^2) - \Sigma_{mR}^{IJ}(m_I^2) \right] + \left. \left[m_I^2 \Sigma_{mL}^{IJ}(m_J^2) - m_J^2 \Sigma_{mL}^{IJ}(m_I^2) \right] \right\} \\ &+ (\Delta F_L)^{IJK}, \end{aligned} \quad (2.9)$$

and $C_R = C_L : (L \leftrightarrow R)$. The parameter η is defined as $\eta^K \equiv Z_R^{2K}/v_2$ with Z_R defined in (A.1). The self energy components obey the following hermicity conditions $\Sigma_{VL(R)}^{JI*} = \Sigma_{VL(R)}^{IJ}$ and $\Sigma_{mL(R)}^{JI*} = \Sigma_{mL(R)}^{IJ}$ and explicitly read in a most compact notation as (S =scalar, F =fermion):

$$\Sigma_{VL}^{IJ}[p, S, F] \equiv \sum_{i,j} V_{uSF,L}^{Iji*} V_{uSF,L}^{Jji} (B_1 + B_0) [p, m_{S_j}, m_{F_i}], \quad (2.10a)$$

$$\Sigma_{mL}^{IJ}[p, S, F] \equiv \sum_{i,j} m_{F_i} V_{uSF,R}^{Iji*} V_{uSF,L}^{Jji} B_0 [p, m_{S_j}, m_{F_i}], \quad (2.10b)$$

with $L \leftrightarrow R$ for Σ_{VR}^{IJ} and Σ_{mR}^{IJ} . Generic vertices V_{uSF} follow the notation of Appendix A.2 in ref. [50]. Explicitly for individual SUSY particles, their forms, copied from ref. [49], are given in Appendix A for complementarity. Detailed definitions for two-point one-loop functions B_0, B_1 are given in Appendix B.

The SUSY-mediated $t \rightarrow qh$ penguin amplitudes can be classified into two distinct topologies: (SFS) squark-gluino/neutralino/chargino-squark and (FSF) chargino/neutralino-squark-chargino/neutralino vertex diagrams. They both contribute to the expressions for the $C_{L,R}^{(h)}$ in (1.2),

$$\Delta F_L = \Delta F_L^{(SFS)} + \Delta F_L^{(FSF)}, \quad (2.11)$$

where in a self-explanatory notation

$$\begin{aligned} \Delta F_L^{(SFS)} &= \Delta F_L^{(\tilde{D}\chi\tilde{D})} + \Delta F_L^{(\tilde{U}\chi^0\tilde{U})} + \Delta F_L^{(\tilde{U}\tilde{g}\tilde{U})}, \\ \Delta F_L^{(FSF)} &= \Delta F_L^{(\chi\tilde{D}\chi)} + \Delta F_L^{(\chi^0\tilde{U}\chi^0)}, \end{aligned} \quad (2.12a)$$

and similar for $\Delta F_R^{(SFS,FSF)}$ with the substitution $L \leftrightarrow R$. Each term in the above expressions will be given by a straightforward substitution in the following compact forms (again explicit vertices for the generalised V 's as well as integral functions can be found in the appendices. External momenta follow the conventions of Fig. 1b:

$$\begin{aligned} \Delta F_L^{(SFS) IJK} &= - \sum_{i,j,l} \left\{ m_I (V_{HSS}^{Kli} V_{uSF,L}^{Ilj*} V_{uSF,L}^{Jij}) (C_{12} - C_{11}) \right. \\ &+ m_J (V_{HSS}^{Kli} V_{uSF,R}^{Ilj*} V_{uSF,R}^{Jij}) (C_{11} + C_0) \\ &+ m_{F_j} (V_{HSS}^{Kli} V_{uSF,R}^{Ilj*} V_{uSF,L}^{Jij}) C_0 \left. \right\} [k_2, k_1, m_{S_i}, m_{S_l}, m_{F_j}], \end{aligned} \quad (2.13a)$$

$$\begin{aligned} \Delta F_L^{(FSF) IJK} &= - \sum_{i,j,l} \left\{ (V_{uSF,R}^{Ijl*} V_{FHF,R}^{iKl} V_{uSF,L}^{Jji}) (\tilde{C}_0 + m_I^2 C_{11} + (m_J^2 - m_I^2) C_{12}) \right. \\ &+ m_I m_J (V_{uSF,L}^{Ijl*} V_{FHF,L}^{iKl} V_{uSF,R}^{Jji}) (C_0 + C_{11}) \\ &+ m_{F_l} m_{F_i} (V_{uSF,R}^{Ijl*} V_{FHF,L}^{iKl} V_{uSF,L}^{Jji}) C_0 \\ &+ m_I m_{F_i} (V_{uSF,L}^{Ijl*} V_{FHF,L}^{iKl} V_{uSF,L}^{Jji}) (C_0 + C_{11} - C_{12}) \\ &+ m_J m_{F_i} (V_{uSF,R}^{Ijl*} V_{FHF,R}^{iKl} V_{uSF,R}^{Jji}) C_{12} \\ &+ m_I m_{F_l} (V_{uSF,L}^{Ijl*} V_{FHF,R}^{iKl} V_{uSF,L}^{Jji}) (C_{11} - C_{12}) \\ &+ m_J m_{F_l} (V_{uSF,R}^{Ijl*} V_{FHF,L}^{iKl} V_{uSF,R}^{Jji}) (C_0 + C_{12}) \left. \right\} [k_1, k_2, m_{S_j}, m_{F_l}, m_{F_i}]. \end{aligned} \quad (2.13b)$$

Again, from these expressions one may also derive the corresponding $\Delta F_R^{(SFS,FSF)}$ by just letting $L \leftrightarrow R$. Integral functions and vertices are given in Appendix A and Appendix B. We have checked both analytically and numerically that the SUSY contributions to $t \rightarrow qh$ amplitudes $C_{L,R}$ are finite and renormalization scale invariant. For our numerical analysis, we have included all the above full expressions into the **SUSY_FLAVOUR** library.

Note that a calculation of the effective Higgs-quark vertices in the MSSM, however without detailed analysis of their phenomenological implications for top quark decays, can also be found in refs. [51, 52]. As discussed there, effects of resummation from higher order chiral corrections are small in the up-quark sector and should not change our qualitative discussion below. However, as such corrections are implemented in `SUSY_FLAVOUR` library, they can indirectly affect those bounds on the flavour changing up-squark Δ parameters which are given by measurements of processes involving down quarks but sensitive to up-squarks circulating in loop amplitudes.

3 $\mathcal{B}(t \rightarrow q h)$: cancellations, decoupling and qualitative results

The formulae given previously, although most general, are quite opaque and do not allow for, at least qualitative, discussion of possible cancellation or enhancement effects taking place in coefficients $C_{L,R}^{(h)}$ of eq. (1.2). We therefore need to perform some approximations.

In the limit where $m_I = m_u(m_c) \rightarrow 0$, the coefficients in (2.9) can be written simply as ($I = 1, 2, J = 3$),

$$C_L^{(h)IJ} = \Delta F_L^{(h)IJ} - \frac{1}{v} \left(\frac{\cos \alpha}{\sin \beta} \right) \Sigma_{mL}^{IJ}(0), \quad (3.1)$$

$$C_L^{(H)IJ} = \Delta F_L^{(H)IJ} - \frac{1}{v} \left(\frac{\sin \alpha}{\sin \beta} \right) \Sigma_{mL}^{IJ}(0), \quad (3.2)$$

with an obvious substitution $L \leftrightarrow R$ for the coefficients $C_R^{(h)}, C_R^{(H)}$. The coefficients that multiply the self energy 1PI diagrams are not simply proportional to $\tan \beta$ as for example is the case for the $\bar{b} s h$ transitions in the MSSM. In the SM limit, where the CP-odd Higgs mass M_A (and therefore the CP-even Higgs boson mass M_H) is taken to be much heavier than M_Z , we have [53]

$$M_A \gg M_Z \quad : \quad \cos \alpha \approx \sin \beta, \quad \sin \alpha \approx -\cos \beta. \quad (3.3)$$

In this case only the decay $t \rightarrow q h$ (i.e., $K = 2$) is relevant and the amplitude is

$$C_L^{(h)IJ} \stackrel{\text{SM limit}}{=} \Delta F_L^{(h)IJ} - \frac{1}{v} \Sigma_{mL}^{IJ}(0), \quad (3.4)$$

with an analogous formula for $C_R^{(h)}$.⁷ In our analytical results for $t \rightarrow q h$ amplitude below, we shall work with the general expressions in eqs. (3.1) and (3.2) and take the SM-limit (3.3) when necessary.

Due to the presence of the strong QCD coupling, gluino diagrams are expected to be dominant. Their contributions can be deduced easily from the general expressions in eqs. (2.10b)

⁷At the moment, LHC data cannot completely exclude [54] but rather *disfavour* [55] the existence of more than one Higgs boson lighter than m_t , with such scenario limited only to certain “tuned” scenarios (see for example ref. [56]).

and (2.13a) and give

$$C_L^{(h_K)IJ} = - \frac{2\alpha_s}{3\pi} \left(\frac{m_t}{m_{\tilde{g}}^2} \right) \sum_{i,l=1}^6 V_{HUU}^{Kli} Z_U^{(J+3)i*} Z_U^{(I+3)l} (C_0 + C_{11}) [\kappa_2, \kappa_1, r_i, r_l, 1] \quad (3.5a)$$

$$+ \frac{2\alpha_s}{3\pi} \left(\frac{1}{m_{\tilde{g}}} \right) \sum_{i,l=1}^6 V_{HUU}^{Kli} Z_U^{Ji*} Z_U^{(I+3)l} C_0 [\kappa_2, \kappa_1, r_i, r_l, 1] \quad (3.5b)$$

$$+ \frac{2\alpha_s}{3\pi} \left(\frac{Z_R^{2K}}{v_2} \right) m_{\tilde{g}} \sum_{i=1}^6 Z_U^{Ji*} Z_U^{(I+3)i} B_0 [0, r_i, 1] , \quad (3.5c)$$

where the first two (ΔF_L) contributions arise from the gluino penguin with flipped chirality in the top quark external line and the gluino internal line respectively, while the last from the self energy (Σ_{mL}), gluino diagram. The symbols in (3.5) are defined in Appendix A. In particular, the mass dimension one, Higgs-squark vertex, V_{HUU}^{Kli} , can be read explicitly from (A.4) and Z_U is the unitary matrix diagonalizing the up-squark mass matrix (see (A.2)), in the basis where quarks are diagonal.⁸ Finally, in (3.5), we have changed to a more suggestive form of Passarino-Veltman (PV) functions with dimensionless parameters, $\kappa_i \equiv k_i/m_{\tilde{g}}$, $r_i \equiv m_i^2/m_{\tilde{g}}^2$, by simply factoring out the gluino mass scale (details of the transformation along with useful properties of the PV functions can be found in Appendix B). Note that in the completely universal case (MFV scenario) where $\kappa_i = 0$ and $r_i = \text{const}$ the whole gluino contribution (3.5) vanishes identically due to unitarity of the Z_U -matrices.

It is interesting to check (3.5) for non-decoupling effects. As we can see from (A.4), the vertex behaves at most as $V_{HUU} \sim M_S$ and therefore, individually, the last two terms in (3.5), do not decouple separately when all SUSY parameters are scaled up by the same factor. However, this non-decoupling behaviour is not realised because of partial cancellations between the penguin and self energy contributions given in (3.5b) and (3.5c), respectively. More specifically, potentially non-decoupled contributions cancel among each other leaving behind remnants with $\sim m_t^2/M_S^2$ as leading behaviour. In this section, we will show this behaviour both numerically, in the full expression, and analytically, up to a certain order in the relevant expansion. For the following quantitative analysis of cancellations and the leading order contributions, it is sufficient to work in the zero external momentum approximation for the penguin and self energy diagrams.

Before proving the cancellations and estimating the behaviour of surviving contributions, we open a parenthesis here to present a useful theorem from matrix algebra. It says the following: consider a Hermitian $n \times n$ matrix A . The trivial decomposition $A = A^0 + \tilde{A}$, where $A^0 = \text{diag}(a_1^0, a_2^0, \dots, a_n^0)$ contains the diagonal elements of A and \tilde{A} contains the non-diagonal elements of A , is always possible. Let the unitary matrix U diagonalizes the matrix A as $U^\dagger A U = D$, where $D = \text{diag}(d_1, d_2, \dots, d_n)$ is a diagonal matrix containing the eigenvalues of matrix A . If we assume that f is an arbitrary analytic function, we can write down the

⁸For more details on the exact definitions of the squark mass and rotation matrices the reader is referred to ref. [49].

following decomposition of matrix $f(A)$ in powers of \tilde{A} matrix elements:

$$\begin{aligned}
[f(A)]_{ij} &= U_{ik} f(d_k) U_{kj}^\dagger = \delta_{ij} f(a_i^0) + \left(\frac{f(a_i^0) - f(a_j^0)}{a_i^0 - a_j^0} \right) \tilde{A}_{ij} + \\
&+ \sum_{\ell=1, (\ell \neq i, j)}^n \left(\frac{\frac{f(a_i^0) - f(a_\ell^0)}{a_i^0 - a_\ell^0} - \frac{f(a_j^0) - f(a_\ell^0)}{a_j^0 - a_\ell^0}}{a_i^0 - a_j^0} \right) \tilde{A}_{i\ell} \tilde{A}_{\ell j} + \dots . \quad (3.6)
\end{aligned}$$

In case of degenerate eigenvalues, the ill-defined ratios in (3.6) should be replaced by appropriate derivatives. The first line of eq. (3.6) has been presented in ref. [57]⁹. A formal proof of eq. (3.6) generalised to all orders in powers of \tilde{A} and its applications to flavour physics will be given elsewhere [58].

For our purpose here, we only require the implementation of eq. (3.6) to the relevant expressions in eq. (3.5). The zero external momentum expansion of self energies and penguins respectively gives (we use here \hat{I}^{IJ} as for a Kronecker “delta” symbol, to avoid confusion with other notation for supersymmetric parameters):

$$\begin{aligned}
\sum_{i=1}^6 Z_U^{Ji*} Z_U^{I+3,i} B_0[0, r_i] &= \hat{\Delta}^{J,I+3} C_0[0; r_J, r_{I+3}, 1] \\
&+ \sum_{K=1}^6 \hat{\Delta}^{JK} \hat{\Delta}^{K,I+3} D_0[0; r_J, r_K, r_{I+3}, 1] \\
&+ \sum_{K,M=1}^6 \hat{\Delta}^{JK} \hat{\Delta}^{KM} \hat{\Delta}^{M,I+3} E_0[0; r_J, r_K, r_M, r_{I+3}, 1] + \mathcal{O}(\hat{\Delta}^4), \quad (3.7a)
\end{aligned}$$

$$\begin{aligned}
\sum_{i,l=1}^6 Z_U^{Ji*} Z_U^{I+3,l} Z_U^{Kl} Z_U^{Ml*} \{C_0, C_{11}\}[0; r_i, r_l, 1] &= \hat{I}^{JK} \hat{I}^{M,I+3} \{C_0, C_{11}\}[0; r_J, r_{I+3}, 1] \\
&+ \hat{I}^{JK} \hat{\Delta}^{M,I+3} \{D_0, D_{11}\}[0; r_J, r_M, r_{I+3}, 1] + \hat{I}^{M,I+3} \hat{\Delta}^{JK} \{D_0, D_{12}\}[0; r_J, r_K, r_{I+3}, 1] \\
&+ \hat{\Delta}^{JK} \hat{\Delta}^{M,I+3} \{E_0, E_{12}\}[0; r_J, r_K, r_M, r_{I+3}, 1] \\
&+ \hat{I}^{JK} \sum_{N=1}^6 \hat{\Delta}^{MN} \hat{\Delta}^{N,I+3} \{E_0, E_{11}\}[0; r_J, r_M, r_N, r_{I+3}, 1] \\
&+ \hat{I}^{M,I+3} \sum_{N=1}^6 \hat{\Delta}^{JN} \hat{\Delta}^{NK} \{E_0, E_{13}\}[0; r_J, r_N, r_K, r_{I+3}, 1] + \mathcal{O}(\hat{\Delta}^3) \quad (3.7b)
\end{aligned}$$

in terms of the diagonal and non-diagonal elements of the dimensionless squark mass matrix

$$r_K^2 \equiv \frac{(\mathcal{M}_U^2)^{KK}}{m_g^2}, \quad \hat{\Delta}^{KM} \equiv \frac{(\mathcal{M}_U^2)^{KM}}{m_g^2} \quad (K \neq M), \quad \hat{\Delta}^{KK} \equiv 0, \quad (3.8)$$

respectively. The quartic product of Z_U matrices in eq. (3.7b) appears after substituting the explicit form of the V_{HUU} vertex in (3.5). The “higher derivative” PV functions D, E

⁹We would like to thank A. Romanino for correspondence on this point.

are defined in Appendix B, together with iterative relations generating them from B and C functions.

An important feature of this “flavour expansion” framework, also noted in ref. [42], is that it allows for a common treatment of completely different flavour structures in \mathcal{M}_U^2 . It may apply with the same efficiency in the “degenerate” case where the diagonal elements r_K are considered to be equal and the mass splitting originates only from $\hat{\Delta}$ or in the “hierarchical” case where the mass splitting from $\hat{\Delta}$ adds to a pre-existing hierarchical pattern in r_K .

Substituting (3.7) into (3.5) in zero external momentum approximation for ΔF_L and using the explicit form of the vertex V_{HUU} from Appendix A, the aforementioned partial cancellations between self-energy and penguin can be seen to take place. While (3.5a) itself has the proper decoupling behaviour, after adding (3.5b) and (3.5c) only few terms survive, remarkably only those with a good decoupling behaviour. After cancellations and in the most general case where the non-holomorphic trilinear couplings A'_U are also present, the scale dependence of the leading remnants in $C_L^{(h)IJ}$, will behave as

$$\begin{aligned}
(3.5b) : & \sim A_U'^{JI} \frac{\cos(\alpha - \beta)}{\sin \beta} \times \mathcal{O}\left(\frac{1}{M_S}\right) & (3.5a) : & \sim \delta_{RR}^{JI} \left(\frac{\cos \alpha}{\sin \beta}\right) \times \mathcal{O}\left(\frac{m_t^2}{M_S^2}\right) \\
& \sim (\mu^* Y^J + A_U'^{JJ}) \delta_{RR}^{JI} \frac{\cos(\alpha - \beta)}{\sin \beta} \times \mathcal{O}\left(\frac{1}{M_S}\right) & & \sim \sum_{A=1}^3 \delta_{RL}^{JA} \delta_{LR}^{AI} \left(\frac{\cos \alpha}{\sin \beta}\right) \times \mathcal{O}(1) \\
& \sim \delta_{LR}^{JI} \left(\frac{\cos \alpha}{\sin \beta}\right) \times \mathcal{O}\left(\frac{m_t}{M_S}\right) \\
& \sim \delta_{LR}^{JJ} \delta_{RR}^{JI} \left(\frac{\cos \alpha}{\sin \beta}\right) \times \mathcal{O}\left(\frac{m_t}{M_S}\right) \\
& \sim \sum_{A,B=1}^3 \delta_{LR}^{JA} \delta_{RL}^{AB} \delta_{LR}^{BI} \left(\frac{\cos \alpha}{\sin \beta}\right) \times \mathcal{O}\left(\frac{M_S}{m_t}\right),
\end{aligned} \tag{3.9}$$

where we have expressed our results in terms of the more useful 3×3 block matrices δ . These are defined through,

$$\hat{\Delta} \equiv \begin{pmatrix} \delta_{LL} & \delta_{LR} \\ \delta_{RL} & \delta_{RR} \end{pmatrix} : \delta_{LR} = (\delta_{RL})^\dagger, \delta_{LL}^{AA} = \delta_{RR}^{AA} = 0, \quad (A = 1, \dots, 3). \tag{3.10}$$

The analytic expressions in (3.9) reveal certain regions in MSSM parameter space where $\mathcal{B}(t \rightarrow q h)$ is enhanced and could be accessible in the high luminosity LHC data. We will investigate these enhanced scenarios in Section 5.

The scaling behaviour of the leading contributions presented in (3.9) is obtained after considering all SUSY mass parameters scaling simultaneously as $\sim M_S$ and all electroweak mass parameters as $\sim m_t$ in the full expression for the leading remnants using (3.6). Under these assumptions the blocks of $\hat{\Delta}$ in eq. (3.10) will behave as

$$\delta_{LL} \sim \delta_{RR} \sim \mathcal{O}(1), \delta_{LR} \sim \mathcal{O}\left(\frac{m_t}{M_S}\right), \tag{3.11}$$

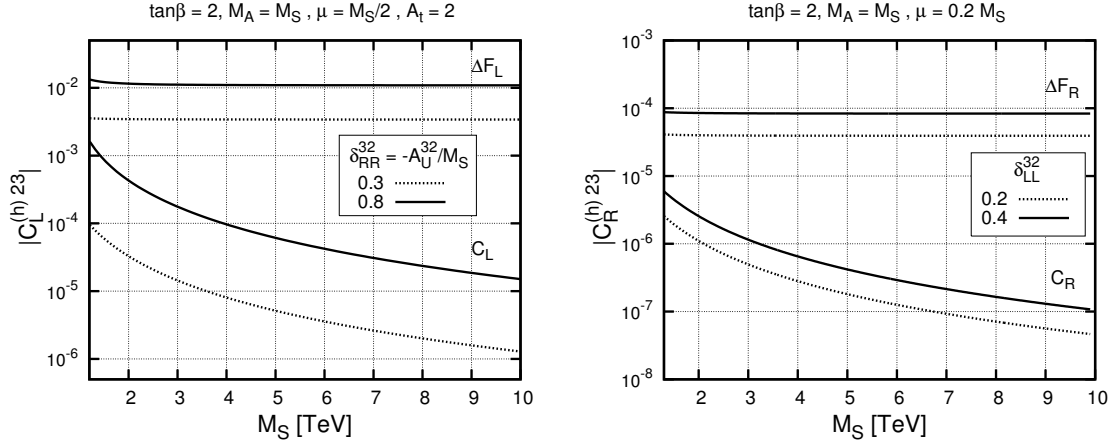


Figure 2: (Left) Cancellation and remnants of $|C_L^{(h)23}|$ for two values of the non-diagonal squark mass parameter δ_{RR}^{32} , assumed here to be related to trilinear term as $\delta_{RR}^{32} = -A_U^{32}/M_S$, in the case of degenerate squark mass spectrum ($r_K^2 = 1$) and a uniform scaling ($M_A = m_{\tilde{g}} = M_S$). The penguin contribution (upper lines) is denoted by (ΔF_L) . (Right) Similarly, for the Wilson coefficient $|C_R^{(h)23}|$ and for two values of δ_{LL}^{32} parameter.

due to the non-uniform scaling of the respective blocks inside \mathcal{M}_U^2 . Using this observation, it is important to notice that all leading remnants in (3.9) scale as $\mathcal{O}(m_t^2/M_S^2)$, which is straightforward to see for all contributions besides the $\sim \cos(\alpha - \beta)$ terms arising from (3.5b). These at first sight seem to exhibit a non-decoupling behaviour, however, a closer look reveals that the decoupling is hidden within the quantity

$$\frac{\cos(\alpha - \beta)}{\sin \beta} \stackrel{\text{SM-limit}}{\simeq} 2 \cos \beta \cos(2\beta) \frac{M_Z^2}{M_A^2} \sim \mathcal{O}\left(\frac{m_t^2}{M_S^2}\right), \quad (3.12)$$

and their contribution can become comparable with all other terms, obviously subject to the $\tan \beta$ value chosen.

The flavour structure of (3.9) may provide us with useful guiding information on the leading dependence of $C_L^{(h)IJ}$ in terms of the Lagrangian parameters involved. For example, for $t \rightarrow ch$ -amplitude [$J = 3, I = 2$ in (3.9)], the parameters directly involved are A_U^{32} , δ_{RR}^{32} and A_U^{32} with the last parameter always introduced through the δ_{LR}^{32} squark mass matrix element. At a secondary level, flavour conserving parameters such as μ or $\delta_{LR}^{33} \sim A_t$ may enter the expressions, however only as pre-factors of the previous ones. As a result they modify substantially the final result of $\mathcal{B}(t \rightarrow ch)$. Analogous results hold for $\mathcal{B}(t \rightarrow uh)$, with obvious superscript replacements $2 \rightarrow 1$ into parameters above.

At this point, it seems instructive to present numerically, in Fig. 2, the cancellation of self energy and penguin contributions in $C_L^{(h)IJ}$ for a typical choice of the parameters involved, and for uniform scaling case $M_A = m_{\tilde{g}} = M_S$ (for the examples illustrated in Fig. 2 we ignore experimental bounds on δ -parameters). We choose to present results in $t \rightarrow ch$ amplitude but analogous results hold also for the $t \rightarrow uh$ amplitude. It is clear from Fig. 2 (left), where we plot the full numerical result for the Wilson coefficient $|C_L^{(h)23}|$ with respect to M_S , that the non-decoupling behaviour of the penguin (ΔF_L) cancels the non-decoupling behaviour of

the self-energy diagrams leaving behind remnants in $|C_L^{(h)23}|$ which are decreasing as m_t^2/M_S^2 . This is scaling behaviour exactly as our approximate expressions in (3.9) indicate.

An analogous situation is realised in Fig. 2(right) in the case of $|C_R^{(h)23}|$ for which, due to the aforementioned $L \leftrightarrow R$ symmetry in the expression for the Wilson coefficients in (3.9), the result primarily depends on δ_{LL}^{32} , $A_U'^{23*}$ and A_U^{23*} . This clear decoupling behaviour is contrary to what has been pointed out recently in ref. [20] about non-decoupling effects due to δ_{LL}^{32} .

One should note that the terms listed in (3.9) are leading or next to leading order contributions in terms of δ -parameters, obtained in the approximation of vanishing momenta of the external particles. Under the uniform scaling of all SUSY parameters these terms scale as $\sim m_t^2/M_S^2$. There are other contributions that scale similarly and can be extracted from the full amplitude expression (3.5). For example, first non-trivial order in the external momentum expansion of the penguin amplitude $\delta F_{L(R)}(k_1, k_2)$ has the similar flavour structure and decoupling properties, so it will modify the coefficients of terms in (3.9) but does not change our qualitative discussion. Other possible terms, e.g. higher order contributions in the flavour expansion, are either subleading in δ 's or small due to other suppression factors, so we do not display them explicitly. They are of course included in the numerical analysis presented in next Sections, as for that we use full unexpanded formulae (2.10) and (2.13).

Finally, similar cancellations of non-decoupling contributions can be observed numerically (and as we checked also analytically, although after more complicated calculations) for chargino and neutralino contributions to the considered $t \rightarrow qh$ decay amplitude. Therefore, they always become smaller than the gluino diagrams, independently of the soft SUSY breaking parameters scale (see also footnote 3).

4 Constraints from other observables

As we discussed already in Section 2 we have added our calculations for $\mathcal{B}(t \rightarrow qh)$ into the `SUSY_FLAVOUR` library [43–45]. For every input MSSM parameter set, `SUSY_FLAVOUR` calculates a number of B -, K -, and D -meson physics observables. Comparing them with experimental bounds [59] allows us to plot predictions for the $t \rightarrow qh$ decay rate only for realistic values of the MSSM parameters.

Most of these observables are related to the processes involving down quarks and they constrain strongly the flavour structure of $m_{Q_L}^2$ soft mass matrix, common from both \tilde{D} and \tilde{U} squarks. Thus, it is unlikely to have $\delta_{LL}^{I3} \gtrsim 10\%$ and this is impossible to generate large effects in $t \rightarrow qh$ decays. We are therefore going to set δ_{LL}^{i3} zero in the numerical results below. For δ_{LR}^{I3} and δ_{RR}^{I3} and at low and moderate values of $\tan\beta$, potentially important constraints for $\mathcal{B}(t \rightarrow qh)$ arise from the D -meson mass difference, ΔM_D . However, ΔM_D is particularly sensitive to δ_{RR}^{12} element, which affects $\mathcal{B}(t \rightarrow qh)$ only through higher powers of δ -insertions than those attributed to the leading effect in (3.9). Also $\mathcal{B}(B \rightarrow X_s \gamma)$ and $\bar{B}_{s(d)} - B_{s(d)}$ mixing could be potentially bound to constraints but they are not significant as contributions from the right up-squark sector to these processes are suppressed by the powers of light quark Yukawa couplings.

There are of course relevant constraints for parameters important for $\mathcal{B}(t \rightarrow qh)$ emerging from direct, mainly LHC, SUSY searches [59, 60]. These are shown in Table 1. A scenario which is particularly interesting for enhancing $\mathcal{B}(t \rightarrow qh)$ is the one with the light stop mostly “right handed”. In this case a lower bound for light stop, together with a nearly degenerate

Quantity	Current Measurement
$m_{\tilde{g}}$	$> 1.1 \text{ TeV}$
single light squark $m_{\tilde{q}}$	$> 500 \text{ GeV}$
$m_{\tilde{t}_L}$	$> 600 \text{ GeV}$
$m_{\tilde{t}_R}$	$> 200 \text{ GeV}$
m_h	$(125.9 \pm 0.4) \text{ GeV}$
Neutron EDM ($ d_n $)	$< 2.9 \cdot 10^{-26} \text{ e cm [63]}$

Table 1: Experimental bounds used throughout in our numerical analysis.

neutralino, as low as $m_{\tilde{t}_R} \approx 200 - 400 \text{ GeV}$ cannot be excluded in current LHC data [60–62].

The recent discovery of the Higgs boson mass at LHC [7,8], if interpreted as an MSSM light Higgs boson, requires a large, often close to maximal, trilinear soft breaking coupling $\delta_{LR}^{33} \propto A_t/M_S \approx \sqrt{6}$. In fact, this helps $\mathcal{B}(t \rightarrow q h)$ to be enhanced as we observe from our qualitative results in (3.9). We have incorporated in **SUSY_FLAVOUR** two-loop approximate expressions for the CP-even Higgs bosons, based on ref. [64] for contributions from the top/stop sector, and supplied with results from ref. [65] for contributions from other sectors. As stated in ref. [64], such approximation should reproduce the full 2-loop result for the Higgs boson mass with accuracy better than 2 GeV. Therefore, we allow for a region $123 \text{ GeV} \lesssim m_h \lesssim 128 \text{ GeV}$, because of unaccounted theory errors from higher loop corrections. Note that full 2-loop formula for the MSSM CP-even Higgs boson mass has not been calculated yet in the fully general flavour violating case, with large off-diagonal squark mass insertion. Thus, actual theoretical error of expressions given in ref. [64] can be bigger, affecting the Higgs mass constraints.

5 Results

Our goal here is to find out the maximal outcome on $\mathcal{B}(t \rightarrow q h)$ in the MSSM. By reading (3.9) the maximal effect on $\mathcal{B}(t \rightarrow q h)$ will be led by the following parameters [FC stands for Flavor Changing and $A_t(A'_t) \equiv A_U^{33}(A_U'^{33})$]:

$$\text{Non - FC : } A_t, \quad A'_t, \quad m_{\tilde{t}_L}, \quad m_{\tilde{t}_R}, \quad \mu, \quad m_{\tilde{g}}, \quad \tan \beta, \quad M_A, \quad (5.1)$$

$$\text{Holomorphic (FC) : } \delta_{LL}^{I3}, \quad \delta_{RR}^{I3}, \quad A_U^{I3}, \quad A_U^{3I}, \quad (5.2)$$

$$\text{Non - Holomorphic (FC) : } A_U'^{I3}, \quad A_U'^{3I}. \quad (5.3)$$

Below we present full numerical results mostly for $\mathcal{B}(t \rightarrow c h)$. This is affected by ($I = 2$) parameters in eqs. (5.2) and (5.3). Results for $\mathcal{B}(t \rightarrow u h)$ are exactly the same as one can see from the leading order expansion (3.9) with the obvious replacement ($I = 1$) in the parameters of eqs. (5.2) and (5.3). Constraints from neutron EDMs are stronger on the latter and as a result we consider mainly $\mathcal{B}(t \rightarrow c h)$ in investigating observability at LHC.

As we have remarked earlier, the analytic formulae, eq. (3.9), allow for the occurrence of enhanced effects in certain regions of parameter space. This saves us from time consuming, and often difficult to understand and interpret, grid-scan plots. Consequently, the following possibilities for an enhanced $\mathcal{B}(t \rightarrow q h)$ emerge.

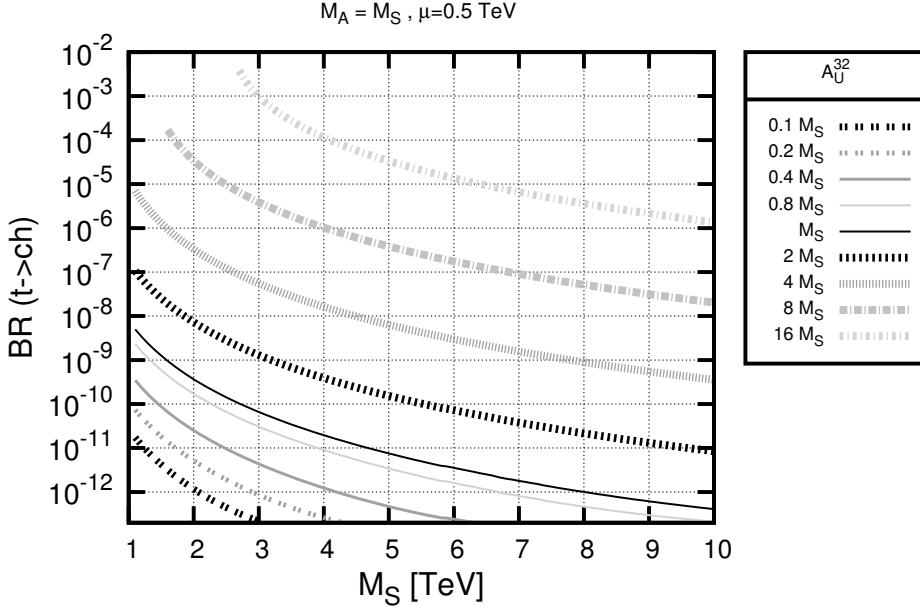


Figure 3: Enhancing the $t \rightarrow ch$ decay rate by varying the A_U^{32} parameter for a degenerate spectrum ($r_K = 1$) and a uniform scaling ($m_{\tilde{g}} = M_A = M_S$). $A_t \approx 2M_S$ and $2 \lesssim \tan \beta \lesssim 4$ are assumed to be consistent with the measured Higgs boson mass of Table 1. The position of the left edge of each line corresponds to the condition $m_{\tilde{t}_L} \geq 600$ GeV.

5.1 Enhancement through large $\frac{|A_U^{31}|}{M_S}$ and $\frac{|A_U^{13}|}{M_S}$

Inspection of (3.9) shows that in leading approximation the expression for $\mathcal{B}(t \rightarrow qh)$ contains several terms depending on up-squark trilinear mixing parameters A_U^{IJ} . The relevant terms in $C_L^{(h)}$ (for $C_R^{(h)}$ one needs to exchange chiral indices $L \leftrightarrow R$) are

$$\begin{aligned}
 C_L^{(h)} : & \sim \delta_{LR}^{JI} \left(\frac{\cos \alpha}{\sin \beta} \right) \mathcal{O} \left(\frac{m_t}{M_S} \right), \quad \sim \sum_{A,B=1}^3 \delta_{LR}^{JA} \delta_{RL}^{AB} \delta_{LR}^{BI} \left(\frac{\cos \alpha}{\sin \beta} \right) \mathcal{O} \left(\frac{M_S}{m_t} \right), \\
 & \sim \sum_{A=1}^3 \delta_{RL}^{JA} \delta_{LR}^{AI} \left(\frac{\cos \alpha}{\sin \beta} \right) \mathcal{O}(1). \quad (5.4)
 \end{aligned}$$

Thus, large A_U^{IJ} values can enhance the discussed decay rates.

Such scenario is illustrated in Fig. 3, where we plot $\mathcal{B}(t \rightarrow ch)$ (so that $J = 3$ and $I = 2$) as a function of $M_S = m_{\tilde{g}} = M_A$ for various values of A_U^{32}/M_S and for a fixed value of $A_t = 2M_S$. In addition, the higgsino mass parameter is set to $\mu = 0.5$ TeV and all other non-diagonal elements of δ vanish. For simplicity in Fig. 3 we vary only A_U^{32}/M_S , setting it to several real-positive values, however as can be seen from analytic formulae, the result for $\mathcal{B}(t \rightarrow ch)$ is symmetric under replacement $A_U^{32} \leftrightarrow A_U^{23}$ and depends primarily on the absolute values of both parameters, so we do not discuss dependence on A_U^{23} separately.

As can be seen from (5.4), the form factor $C_L^{(h)}$ contain terms with linear dependence and a term with cubic dependence in $\delta_{LR}^{32} = -\frac{v_2 A_U^{32}}{\sqrt{2} M_S^2}$. Linear dependence dominates for

$A_U^{32}/M_S \ll 1$ while, more importantly, cubic dependence dominates for $A_U^{32}/M_S \gg 1$. As it is obvious from second line of (5.4), the parameter $A_t \approx 2M_S$, required for a 126 GeV Higgs boson mass, enhances $|C_L|$ and therefore $\mathcal{B}(t \rightarrow ch)$, only in parameter regions where linear dependence dominates, namely for $A_U^{32}/M_S \ll 1$. In the more interesting cubic dependence region, where $A_U^{32}/M_S \gg 1$ and the maximal values of $\mathcal{B}(t \rightarrow ch)$ are obtained, the branching ratio can reach LHC attainable values, exceeding estimate (1.7) by two orders of magnitude, for $A_U^{32} \gtrsim 8M_S$ and for a light M_S value, as can be seen in the left upper corner of Fig. 3. There, the minimum value of M_S is subject to the condition that the left handed stop squark mass is heavier than 600 GeV, as Table 1 indicates.

We should note that our results for $\mathcal{B}(t \rightarrow ch)$ shown in Fig. 3 do not display any non-decoupling effect. The decay rate increases with the A_U^{32}/M_S ratio, but for each fixed choice of A_U^{32}/M_S it decreases as our analytic formulae indicate, *i.e.*, as $|C_L|^2 \sim m_t^4/M_S^4$. In the most interesting region $A_U^{32}/M_S \gg 1$, where the cubic dependence in δ_{LR}^{32} dominates C_L , the branching ratio behaves as

$$\mathcal{B}(t \rightarrow ch) \propto \left(\frac{A_U^{32}}{M_S}\right)^6 \mathcal{O}\left(\frac{m_t^4}{M_S^4}\right). \quad (5.5)$$

A small deviation from this behaviour can be seen on the left edge of the upper curves where steeper slopes appear due to $|\delta_{LR}^{32}|$ closing to unity and higher order corrections becoming increasingly important. For large M_S , deep in the SM (decoupling)-limit, although the effect is substantially smaller, the $\mathcal{B}(t \rightarrow ch)$ is still enhanced by many orders of magnitude as compared to the SM prediction.

Another important remark should be done concerning how realistic are very large values of $|A_U^{32}|/M_S$ (or $|A_U^{23}|/M_S$), required to enhance the $\mathcal{B}(t \rightarrow ch)$. As previously mentioned, they are always constrained by the condition $|\delta_{LR}^{32(23)}| \lesssim 1$ resulting from the light stop mass bound:

$$|\delta_{LR}^{32}| \sim \frac{v_2}{\sqrt{2}M_S} \frac{|A_U^{32}|}{M_S} \lesssim 1 \quad \longrightarrow \quad \frac{|A_U^{32}|}{M_S} \lesssim \frac{\sqrt{2}M_S}{v_2}. \quad (5.6)$$

Thus, in principle even very large values of $|A_U^{32}|/M_S$ are possible assuming sufficiently high SUSY mass scale, e.g. for $M_S > 1.5$ TeV one can reasonably consider $A_U^{32} \sim 8M_S$. However, such large A_U in connection with light stop mass square can possibly trigger unwanted Charge and Colour Breaking minima (CCB) [66–77]. For example, allowing for non-vanishing A_U^{32} and following the steps of ref. [68], and assuming possible vevs in the five dimensional field space direction, $H_1^0 = 0, H_2^0 = 1, \tilde{t}_L = 0, \tilde{t}_R = \tilde{c}_R = 1$,¹⁰ we arrive analytically at the following constraint,

$$|A_U^{32}|^2 \leq Y_t^2 (m_{H_2}^2 + m_{\tilde{t}_L}^2 + m_{\tilde{c}_R}^2 + \mu^2), \quad (5.7)$$

in agreement with ref. [72]. One can arrive at an even stronger bound involving both $|A_t|$ and $|A_U^{32}|$, which is appreciable because of the Higgs mass constraint, following the field direction $\tilde{t}_L = H_2^0 = 1, H_1^0 = 0, \tilde{t}_R = \tilde{c}_R = 1/\sqrt{2}$,

$$(|A_t| + |A_U^{32}|)^2 \leq 4 Y_t^2 [m_{H_2}^2 + m_{\tilde{t}_L}^2 + \frac{1}{2}(m_{\tilde{t}_R}^2 + m_{\tilde{c}_R}^2)]^2, \quad (5.8)$$

in agreement with a similar one found recently in ref. [78]. For a common squark and Higgs mass scale, M_S , the constraint (5.7) results in $|A_U^{32}| \lesssim \sqrt{3}M_S$, which is far more stringent

¹⁰Fields are normalized to H_2^0 and we take the limit, $Y_c^2/Y_t^2 \rightarrow 0$.

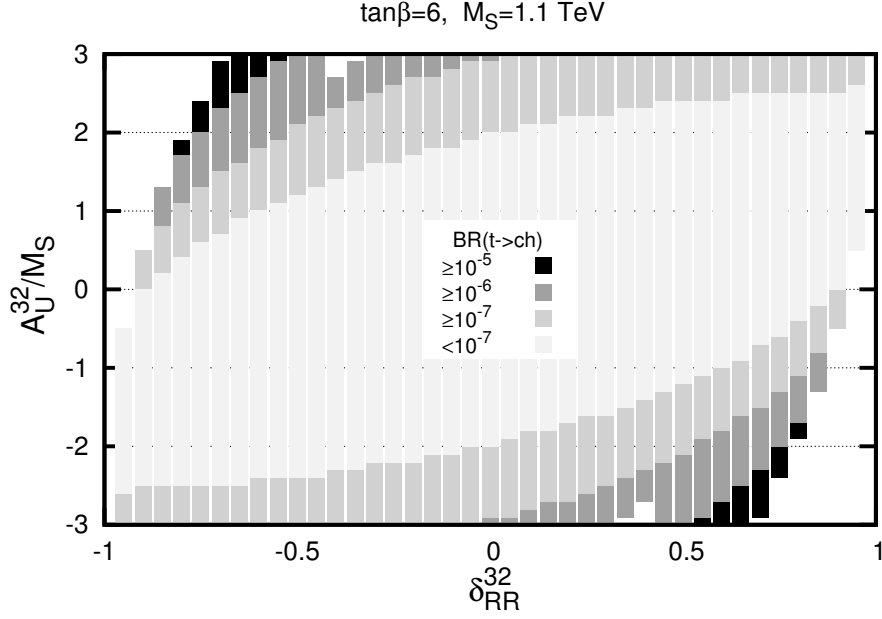


Figure 4: Contour plot for $\mathcal{B}(t \rightarrow ch)$ prediction on a δ_{RR}^{32} vs. A_U^{32}/M_S plane. All other FC parameters are set to zero. In addition, we take $(m_{\tilde{g}} = M_A = \mu = M_S)$ and $A_t/M_S = 2$ while other values are shown in the figure.

than the positivity physical mass squared constraint of (5.6). For such values of A_U^{32} , and, after reading from Fig. 3, we deduce that

$$\mathcal{B}(t \rightarrow ch) \lesssim 10^{-7}. \quad (5.9)$$

This rate is out of any near future LHC expected sensitivity [see (1.4)].

A detailed analysis of the CCB problem in the general flavour violating MSSM is beyond the scope of this paper. Nevertheless, in most cases the issue is a cosmological one, since sometimes the inverse transition rate between meta-stable vacua exceeds the lifetime of the universe. In this case, the pre-factor of $\mathcal{O}(1)$ in the RHS of eq. (5.7) may be modified, but it is unlikely that it increases by an order of magnitude or so, necessary to achieve $\mathcal{B}(t \rightarrow ch) \sim 10^{-4}$. This claim is supported by the results of ref. [74], where the bound in eq. (5.7) is only marginally relaxed by meta-stability. For recent accounts on meta-stability of the MSSM vacuum in MFV scenario, see refs. [75–77].¹¹

In a more general case both A_U^{32} and δ_{RR}^{32} parameters can be present simultaneously. In this case the possibly largest contributions to the $C_L^{(h)}$ form factor, out of all listed in (3.9), are given by terms

$$\sim \delta_{LR}^{JJ} \delta_{RR}^{JI} \left(\frac{\cos \alpha}{\sin \beta} \right) \times \mathcal{O} \left(\frac{m_t}{M_S} \right), \quad \sim \delta_{LR}^{JI} \delta_{RL}^{IJ} \delta_{LR}^{JI} \left(\frac{\cos \alpha}{\sin \beta} \right) \times \mathcal{O} \left(\frac{M_S}{m_t} \right). \quad (5.10)$$

¹¹A more robust check for CCB vacua can be studied with the publicly available code **Vevacious** [79] which performs a full numerical check of the potential (meta)stability even at 1-loop level. A thorough scan of the interesting parameter space can be however limited by long computer run-time.

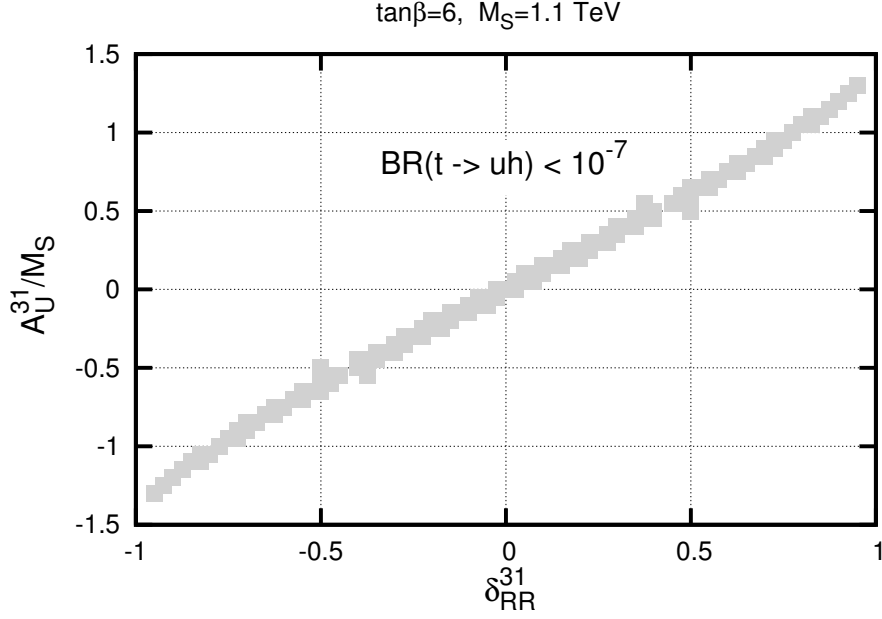


Figure 5: Contour plot for $\mathcal{B}(t \rightarrow uh)$ on a δ_{RR}^{31} vs. A_U^{31}/M_S plane with all other parameters set as in Fig. 4. Due to severe neutron EDM constraints, the effect is confined to a region where the decay rate is far beyond the reach of LHC.

In Fig. 4 we plot $\mathcal{B}(t \rightarrow ch)$ on the δ_{RR}^{32} and A_U^{32}/M_S plane, varying A_U^{32} within the region $|A_U^{32}|/M_S \lesssim 3$ in order to avoid potential CCB bounds. Note that contributions from these two parameters can interfere constructively (top-left and bottom-right corners of the plot) or destructively (bottom-left and top-right corners). However, even in the most optimistic case, the branching ratio $\mathcal{B}(t \rightarrow ch)$ cannot exceed values of order $\sim 10^{-5}$ which is an order of magnitude less than the expected sensitivity of LHC.

An analogous effect for $\mathcal{B}(t \rightarrow ch)$ may also arise from the $C_R^{(h)}$ contribution, namely from the A_U^{23*} and δ_{LL}^{32} pair of parameters. However including such an effect has little to offer since the enhancement that could be obtained this way (factor 2 at most) is suppressed due to the stringent experimental bounds on δ_{LL} .

In Fig. 5 we present results for $\mathcal{B}(t \rightarrow uh)$ on a δ_{RR}^{31} vs. A_U^{31}/M_S plane. As we have already discussed, formulae for this decay are exactly the same as for $\mathcal{B}(t \rightarrow ch)$, with obvious replacements of indices of flavour violating parameters. However, the important difference comes from the fact that A_U^{31} , A_U^{13} and δ_{RR}^{13} are highly constrained by experimental bound on neutron Electric Dipole Moment (EDM), see e.g. [80]. Although we have assumed *real* parameters throughout this article, this is an effect that arises from the terms of the higher order in the mass insertion expansion of the gluino contribution to the down quark electric and chromoelectric dipole moments. Such terms are proportional to $A_U^{31(13)}$ or δ_{RR}^{13} multiplied by the CKM matrix elements containing imaginary phase. Effects of this kind are usually quite small and unobservable, comparing to experimental and theoretical accuracy with which most of the rare processes is known. However, the bound on neutron EDM is so strong, that it has visible impact on the acceptable ranges of the real soft parameters. Approximately, the whole effect results in a strong correlation of the allowed values of A_U^{31}/M_S and δ_{RR}^{31} , such that

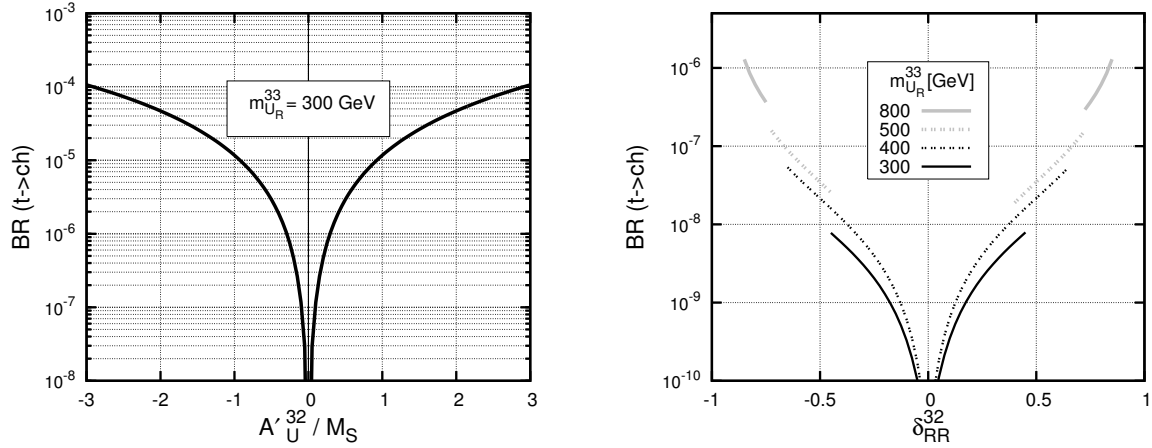


Figure 6: Branching ratios for the light $M_A = 110$ GeV scenario and chosen set of MSSM parameters: $\tan \beta = 6$, $\mu = 250$ GeV, $M_S = 1.1$ TeV, $A_t/M_S = 2.7$. The leading contribution (left panel) originates from the non-holomorphic coupling A_U^{32} . If $A_U^{32} \approx 0$ the next to leading contribution (right panel) is controlled by $(\mu^* \delta_{RR}^{32})$. The allowed δ_{RR}^{32} range for each $m_{U_R}^{33}$ value corresponds to the $200 < m_{\tilde{t}_R} < 400$ GeV constraint of the “light stop window” [61].

their linear combination with $\mathcal{O}(1)$ coefficients (depending on up-squark and gluino masses) must vanish with $\mathcal{O}(10^{-2})$ accuracy, to satisfy the current experimental neutron EDM bound in Table 1. As it is obvious from Fig. 5, we then find $\mathcal{B}(t \rightarrow u h) \lesssim 10^{-7}$ which is unobservable at LHC.

Based on (3.9), one can in principle search how to enhance $\mathcal{B}(t \rightarrow q h)$ other than by previously analysed its cubic dependence on A_U^{32}/M_S . An analogous effect may also be produced by increasing $\sim \delta_{RR}^{32}$ together with the unnatural choice of $|\mu|/M_S \gg 1$. Even so, such a contribution is suppressed by the condition $\delta_{RR}^{32} < 1$ and thus will be typically subleading, unless $\mu/M_S \gg A_U^{32}/M_S$. Therefore, the parameter space exploited in Figs. 3 and 4 seems to be the optimal one.

5.2 The light M_A scenario and non-holomorphic dominance

The second enhancement scenario requires a light Higgs sector and significant contribution from the non-holomorphic trilinear soft couplings, A_U' . The numerical results are displayed in Fig. 6. We shall attempt here an explanation of the enhancement based on analytic expansion in (3.9). We must warn the reader however that this case scenario disfavoured by LHC data and we mostly present it here for complementarity reasons.

This scenario departs from the assumption of uniform scaling for M_A and assume light $M_A \sim M_Z$. Only terms proportional to $\cos(\alpha - \beta)$ in (3.5a), (3.5b) will be enhanced [see also eq. (3.12)]. To illustrate the size of possible light M_A effects we assume for simplicity vanishing non diagonal squark mass matrix elements beside $A_U'^{23}$ and δ_{RR}^{32} in left and right panels of Fig. 6, respectively. In order to make this point quantitative, we follow the scenario of ref. [56] in which the heavy Higgs boson is the one seen at LHC with mass around 125.5 GeV and the light one lies in the region $95 \lesssim m_h \lesssim 101$ GeV where LEP had seen some small excess in Higgs data.

As we observe from the left panel of Fig. 6, the non-holomorphic soft breaking term $A_U^{23} \approx 3M_S$ may easily bring $\mathcal{B}(t \rightarrow ch)$ to the level observable in future LHC measurements. This is not true in the right panel of Fig. 6, where δ_{RR}^{32} is varied instead. Here effect is much smaller due to the constraints $\delta_{RR}^{32} < 1$ (physical squark masses) and $|\mu| < 400$ GeV ($b \rightarrow s\gamma$). In that case we obtain $\mathcal{B}(t \rightarrow ch) \lesssim 10^{-6}$, far off LHC's future sensitivity.

Also the more promising scenario with enhanced non-holomorphic contribution in Fig. 6 (left panel) can only be realised in particular parameter choice. In such a scenario, the $B \rightarrow X_s \gamma$ constraint imposes $\mu \lesssim 400$ GeV. One of the two charginos, namely the higgsino-like one, with mass proportional to μ , should be light and cancel the charged Higgs terms in the respective penguin diagrams. Thus we choose μ small and heavy winos in order to split the chargino masses. We have also taken a tuned value for trilinear SUSY breaking coupling, $A_t/M_S = 2.7 \pm 0.05$, which allows to pass the constraints of Table 1 and $B \rightarrow X_s \gamma$, for a large region in μ , namely $150 < |\mu| < 350$ GeV. We could relax the tuning here but only at the cost of severely restricting the μ parameter space, $\mu \simeq (125 \sim 150)$. In any case $|A_t/M_S| \simeq (2 \sim 3)$ is always required in this scenario. Finally, following ref. [56] we can only vary $\tan \beta$ within the $\tan \beta \simeq 6 \sim 7$ region.

In the light of recent searches for charged Higgs boson produced in $t \rightarrow H^+ b$ decays and decaying to τ 's [55] this scenario seems increasingly unlikely, at least assuming MSSM relations between the Higgs boson masses. In principle, there is an open window (at 1σ) around $6 \lesssim \tan \beta \lesssim 10$ but only at very low m_{H^\pm} masses less than 110 GeV. Using the MSSM Higgs boson mass sum rule $m_{H^\pm}^2 = m_A^2 + m_W^2$, this would require very light $M_A \lesssim 75$ GeV far below $M_A = 110$ GeV suggested by the LEP possible excess.

6 Conclusions

In the present article we have studied rare, flavour-changing top quark decays to light up quarks u or c and the Higgs boson h ,

$$t \rightarrow uh \quad \text{or} \quad t \rightarrow ch,$$

in the framework of MSSM with R -parity conservation. Although the corresponding processes in the framework of the Standard Model are highly suppressed, mostly due to the GIM mechanism, such a suppression is not a priori expected in the case of MSSM.

We improve upon existed calculations, most notably from refs. [16–18], by including next to leading order QCD corrections and RGE running from the SUSY soft breaking masses down to m_t . SUSY finite threshold effects into $t \rightarrow qg$ that mixes with $t \rightarrow qh$, are fully included. This set of most up-to-date one-loop corrections to $t \rightarrow qh$ amplitudes are then included in publicly available **SUSY FLAVOUR** library, and therefore combined with MSSM predictions from numerous other flavour physics observables. In addition to current literature, we study effects arising from the non-holomorphic soft SUSY breaking terms. These turn out to be important for enhancing $\mathcal{B}(t \rightarrow qh)$ but in a parameter region already disfavoured by LHC.

Moreover, we have obtained an analytical expansion of the dominant gluino amplitude by using a theorem of matrix algebra [58] and have arrived at the approximate master formula (3.9). This formula worked as a guide in order to understand better the cancellations between various contributions, decoupling effects and enhancement scenarios in $t \rightarrow qh$ amplitude. We conclude that the main enhancement for $\mathcal{B}(t \rightarrow ch)$ arises basically from the largeness of the parameters: $|\delta_{LR}^{32}| \sim |A_U^{32}|/M_S$ (and/or $|\delta_{RL}^{32}|$) and $|\delta_{RR}^{32}|$.

Numerical results depicted in Figs. 3 and 4 show that for $|A_U^{32}|/M_S \gtrsim O(1)$ or $|\delta_{RR}^{32}| \sim O(1)$, the branching ratio $\mathcal{B}(t \rightarrow ch) \approx 10^{-5}$ is enhanced almost by 9 orders of magnitude w.r.t. SM expectation, but unfortunately it is still below the near future LHC sensitivity of (1.4). This is because of cancellations between leading order penguin and self energy diagrams, so that decoupling always takes place. Only in case where $|A_U^{32}| \gtrsim 8M_S$ the branching ratio is approaching the expected LHC sensitivity. In such a case however CCB minima are likely to appear as we briefly showed in eq. (5.7) or (5.8).

For $t \rightarrow uh$ on the other hand, although in principle the decay rate is expected to be of the same order as with $t \rightarrow ch$, the neutron EDM constraints, induced from the CKM phase, severely suppress the allowed parameter space into a tuned region in which decay rates are small, $\mathcal{B}(t \rightarrow uh) < 10^{-7}$, again far below experimental sensitivity.

We therefore conclude that an MSSM driven $\mathcal{B}(t \rightarrow qh)$ is unlikely to be observed even at high luminosity LHC. Apart from rather unnatural corners of the parameter space, the typical MSSM prediction, even for flavour changing insertions in the up sector of $\delta_{LR,RR} \sim \mathcal{O}(1)$, is $\mathcal{B}(t \rightarrow qh) \approx 10^{-8} - 10^{-9}$. Although small, this is still five to six orders of magnitude above the SM expectation. If LHC discovers up-squarks and gluinos it will be vital to develop techniques that will take us to such small branching ratios for $t \rightarrow qh$ decay. If however LHC observes the rare $t \rightarrow qh$ decays at projected maximal sensitivity of about 10^{-4} , their origin must probably lie in physics other than, or beyond, MSSM with R-parity conservation.

Acknowledgements

AD would like to thank Francesca Borzumati, Sven Heinemeyer and Howie Haber for useful discussions during SUSY-2014 conference. We would like to thank Wolfgang Altmannshofer for bringing to our attention refs. [72, 74, 78] for CCB constraints on flavour changing mass insertions. This research has been co-financed by the European Union (European Social Fund - ESF) and Greek national funds through the Operational Program “Education and Lifelong Learning” of the National Strategic Reference Framework (NSRF) - Research Funding Program: THALIS-Investing in the society of knowledge through the European Social Fund. J.R. would like to thank University of Ioannina and CERN for the hospitality during his stays there. His work was supported in part by the Polish National Science Center under the research grants DEC-2011/01/M/ST2/02466 and DEC-2012/05/B/ST2/02597.

Appendix A Explicit expressions for MSSM vertices

Throughout the paper we follow the notation and conventions of refs. [48, 49], where the definitions of the Lagrangian parameters, mass matrices and mixing matrices used for their diagonalization are given for all MSSM sectors. Here for completeness we repeat just the explicit expressions for the couplings needed to calculate the effective $t \rightarrow q h$ vertex in Section 2. For more details the reader is referred to more up-to-date ref. [49].

The CP-even Higgs boson mass rotation matrix Z_R is defined in terms of commonly used angle- α as (also as usual $\tan \beta = \frac{v_2}{v_1}$)

$$Z_R = \begin{pmatrix} \cos \alpha & -\sin \alpha \\ \sin \alpha & \cos \alpha \end{pmatrix}. \quad (\text{A.1})$$

Matrices used to mass matrices of supersymmetric particles are defined, respectively, as:

$$\begin{aligned} Z_-^T M_C Z_+ &= \text{diag}(m_{\chi_1}, m_{\chi_2}) && \text{chargino}, \\ Z_N^T M_N Z_N &= \text{diag}(m_{\chi_1^0}, \dots, m_{\chi_4^0}) && \text{neutralino}, \\ Z_D^\dagger M_D^2 Z_D &= \text{diag}(m_{D_1}^2, \dots, m_{D_6}^2) && \text{down squarks}, \\ Z_U^T M_U^2 Z_U^* &= \text{diag}(m_{U_1}^2, \dots, m_{U_6}^2) && \text{up squarks}, \end{aligned} \quad (\text{A.2})$$

where the expressions for M_C, M_N, M_D^2, M_U^2 can be found in ref. [49].

With the above definitions, relevant tree-level vertices can be written down as (summation from 1 to 3 over all repeating flavour indices A, B, \dots is always assumed):

- Neutral CP-even Higgs-up quark coupling is:

$$V_{uHu}^{IKI} = -\frac{1}{\sqrt{2}} Y_u^I Z_R^{2K}, \quad (\text{A.3})$$

where up-quark Yukawa coupling is $Y_u^I = \frac{\sqrt{2}m_u^I}{v_2}$.

- Couplings relevant for diagram with gluino exchange:

$$\begin{aligned} V_{HUU}^{Kli} &= -\frac{e^2}{3c_W^2} (v_1 Z_R^{1K} - v_2 Z_R^{2K}) (\hat{I}^{li} + \frac{3 - 8s_W^2}{4s_W^2} Z_U^{Al*} Z_U^{Ai}) \\ &\quad - v_2 (Y_u^A)^2 Z_R^{2K} (Z_U^{Al*} Z_U^{Ai} + Z_U^{(A+3)l*} Z_U^{(A+3)i}) \\ &\quad + \frac{1}{\sqrt{2}} Z_R^{2K} (A_u^{AB*} Z_U^{Al*} Z_U^{(B+3)i} + A_u^{AB} Z_U^{Ai} Z_U^{(B+3)l*}) \\ &\quad + \frac{1}{\sqrt{2}} Z_R^{1K} (A_u'^{AB*} Z_U^{Al*} Z_U^{(B+3)i} + A_u'^{AB} Z_U^{Ai} Z_U^{(B+3)l*}) \\ &\quad + \frac{1}{\sqrt{2}} Y_u^A Z_R^{1K} (\mu^* Z_U^{Ai} Z_U^{(A+3)l*} + \mu Z_U^{Al*} Z_U^{(A+3)i}), \end{aligned} \quad (\text{A.4})$$

$$V_{uU\tilde{g},L}^{Jji} = g_3 \sqrt{2} T_{ab}^i (-Z_U^{Jj*}), \quad (\text{A.5})$$

$$V_{uU\tilde{g},R}^{Iji} = g_3 \sqrt{2} T_{ab}^i (Z_U^{(I+3)j*}), \quad (\text{A.6})$$

where the generators T^i are the Gell-Mann of SU(3) with Casimir invariant normalised to $C^2 = \sum_j T^j T^j = \frac{4}{3} \hat{\mathbf{I}}$.

- Additional couplings necessary for neutralino mediated diagrams are:

$$V_{\chi^0 H \chi^0, L}^{lKi} = V_{\chi^0 H \chi^0, R}^{iKl*} = \frac{e}{2s_W c_W} \left((Z_R^{1K} Z_N^{3i} - Z_R^{2K} Z_N^{4i})(Z_N^{1l} s_W - Z_N^{2l} c_W) \right. \\ \left. + (Z_R^{1K} Z_N^{3l} - Z_R^{2K} Z_N^{4l})(Z_N^{1i} s_W - Z_N^{2i} c_W) \right), \quad (\text{A.7})$$

$$V_{uU \chi^0, L}^{Jji} = \frac{-e}{\sqrt{2}s_W c_W} Z_U^{Ij*} \left(\frac{1}{3} Z_N^{1i} s_W + Z_N^{2i} c_W \right) - Y_u^I Z_U^{(I+3)j*} Z_N^{4i}, \quad (\text{A.8})$$

$$V_{uU \chi^0, R}^{Iji} = \frac{2\sqrt{2}e}{3c_W} Z_U^{(I+3)j*} Z_N^{1i*} - Y_u^I Z_U^{Ij*} Z_N^{4i*}, \quad (\text{A.9})$$

- Couplings relevant for chargino mediated diagrams are:

$$V_{\chi H \chi, L}^{lKi} = V_{\chi H \chi, R}^{iKl*} = -\frac{e}{\sqrt{2}s_W} \left(Z_R^{1K} Z_-^{2i} Z_+^{1l} + Z_R^{2K} Z_-^{1i} Z_+^{2l} \right), \quad (\text{A.10})$$

$$V_{uD \chi, L}^{Jji} = -\left(\frac{e}{s_W} Z_D^{Aj} Z_-^{1i} + Y_d^A Z_D^{A+3j} Z_-^{2i} \right) K^{JA*}, \quad (\text{A.11})$$

$$V_{uD \chi, R}^{Iji} = Y_u^I Z_D^{Aj} Z_+^{2i*} K^{IA*}, \quad (\text{A.12})$$

$$V_{HDD}^{Kli} = \frac{e^2}{6c_W^2} (v_1 Z_R^{1K} - v_2 Z_R^{2K}) (\hat{I}^{li} + \frac{3-4s_W^2}{2s_W^2} Z_D^{Al*} Z_D^{Ai}) \\ - v_1 (Y_d^A)^2 Z_R^{1K} (Z_D^{Al*} Z_D^{Ai} + Z_D^{(A+3)l*} Z_D^{(A+3)i}) \\ - \frac{1}{\sqrt{2}} Z_R^{1K} (A_d^{AB*} Z_D^{Ai} Z_D^{(B+3)l*} + A_d^{AB} Z_D^{Al*} Z_D^{(B+3)i}) \\ + \frac{1}{\sqrt{2}} Z_R^{2K} (A_d'^{AB*} Z_D^{Ai} Z_D^{(B+3)l*} + A_d'^{AB} Z_D^{Al*} Z_D^{(B+3)i}) \\ - \frac{1}{\sqrt{2}} Y_d^A Z_R^{2K} (\mu^* Z_D^{Al*} Z_D^{(A+3)i} + \mu Z_D^{Ai} Z_D^{(A+3)l*}). \quad (\text{A.13})$$

where K is the Cabibbo-Kobayashi-Maskawa matrix and $Y_d^I = -\frac{\sqrt{2}m_d^I}{v_1}$.

One should also note that the conventions used in the paper, following refs. [48, 49] differ minimally from the now commonly accepted SLHA2 convention [81] for the MSSM parameters. However, translation of the soft breaking parameters (others do not differ at all) can be done immediately using the Table 2.

SLHA2 [81]	Ref. [48, 49]
$\hat{T}_U, \hat{T}_D, \hat{T}_E$	$-A_u^T, +A_d^T, +A_l^T$
$\hat{m}_{\tilde{Q}}^2, \hat{m}_{\tilde{L}}^2$	m_Q^2, m_L^2
$\hat{m}_{\tilde{u}}^2, \hat{m}_{\tilde{d}}^2, \hat{m}_{\tilde{l}}^2$	$(m_U^2)^T, (m_D^2)^T, (m_E^2)^T$
$\mathcal{M}_{\tilde{u}}^2, \mathcal{M}_{\tilde{d}}^2$	$(\mathcal{M}_U^2)^T, (\mathcal{M}_D^2)^T$

Table 2: Comparison of SLHA2 [81] and Refs. [48, 49] conventions.

Appendix B Passarino-Veltman loop functions

Our convention for Passarino-Veltman integral functions follows Axelrod's in ref. [82]. For the integrals entering directly our 1PI-irreducible amplitudes, we have the defining expressions for 2- and 3-point functions:

$$\{B_0, B^\mu\}[k_1, m_1, m_2] \equiv \int \frac{d^4 p}{(2\pi)^4} \frac{\{1, p^\mu\}}{(p^2 - m_1^2)((p + k_1)^2 - m_2^2)} , \quad (\text{B.1})$$

$$\{C_0, C^\mu, \tilde{C}_0\}[k_1, k_2, m_1, m_2, m_3] \equiv \int \frac{d^4 p}{(2\pi)^4} \frac{\{1, p^\mu, p^2\}}{(p^2 - m_1^2)((p + k_1)^2 - m_2^2)((p + k_1 + k_2)^2 - m_3^2)} . \quad (\text{B.2})$$

The expression above can be generalised to the case of general n -point 1-loop functions as:

$$PV_n^{\mu_1 \dots \mu_l}[k_1, \dots, k_{n-1}, m_1, \dots, m_n] = \int \frac{d^4 p}{(2\pi)^4} \frac{p^{\mu_1} \dots p^{\mu_l}}{(p^2 - m_1^2) \prod_{j=2}^n ((p + k_1 + \dots + k_{j-1})^2 - m_j^2)} , \quad (n \geq 2) . \quad (\text{B.3})$$

Obviously, for $n = 2, 3$ one obtains the analytic expression for the B, C -functions given in eqs. (B.1) and (B.2) (with $\tilde{C}_0 = g_{\mu\nu} PV_3^{\mu\nu}$). In standard notation higher order $n = 4, 5 \dots$ functions are commonly denoted as D, E, \dots -functions. Such higher order integrals are absent from the calculation of $t \rightarrow q h$ decays at one-loop [eqs. (2.10) and (2.13)], but they unavoidably arise in the flavour expansion approximation of eq. (3.7).

In practical calculations, it is usually more convenient to replace the tensorial integral functions by functions transforming as scalars under the Lorentz group. For the lowest vectorial functions they are defined through the relation

$$B^\mu = k_1^\mu B_1 , \quad [k_1, m_1, m_2] \quad (\text{B.4})$$

$$C^\mu = k_1^\mu C_{11} + k_2^\mu C_{12} , \quad [k_1, k_2, m_1, m_2, m_3] \quad (\text{B.5})$$

...

$$PV_n^\mu = k_1^\mu \overline{PV}_n^1 + \dots + k_{n-1}^\mu \overline{PV}_n^{n-1} = \sum_{i=1}^{n-1} k_i^\mu \overline{PV}_n^i , \quad [k_1 \dots k_{n-1}; m_1 \dots m_n] \quad (\text{B.6})$$

and similarly for higher tensor functions. In our notation, all arguments, common for PV-functions of equal order n , are displayed separately within the respective brackets.

For FC processes, where partial cancellations between topologically distinct diagrams take place, it is considerably more convenient to work in a different description of the PV-functions in which all arguments become dimensionless. As follows directly from the definition (B.3), PV loop integrals are homogeneous functions of their arguments:

$$PV_n^{\mu_1 \dots \mu_l}[k_1, \dots, k_{n-1}, m_1, \dots, m_n] = M^{4+l-2n} PV_n^{\mu_1 \dots \mu_l} \left[\frac{k_1}{M}, \dots, \frac{k_{n-1}}{M}, \frac{m_1}{M}, \dots, \frac{m_n}{M} \right] ,$$

with M being an arbitrary mass scale, usually chosen as a typical scale for a given loop diagram.

A useful property associates differences of integral functions of a certain order with integral functions of next order. For example, as can be directly verified from the definitions in eqs. (B.1) and (B.2), one has

$$\frac{B_0[k_1, m_1, M_2] - B_0[k_1, m'_1, M_2]}{m_1^2 - m'^2_1} = C_0[0, k_1, m_1, m'_1, M_2] . \quad (\text{B.7})$$

In general case this relation has the following structure:

$$\begin{aligned} \frac{PV_n^X[k_1 \dots k_{n-1}; m_1 \dots M_n] - PV_n^X[k_1 \dots k_{n-1}; m'_1 \dots M_n]}{m_1^2 - m'^2_1} \\ = PV_{n+1}^X[0, k_1 \dots k_{n-1}; m_1, m'_1 \dots M_n] , \end{aligned} \quad (\text{B.8})$$

$$\begin{aligned} \frac{PV_n^X[\dots k_{j-1} \dots; \dots m_j \dots] - PV_n^X[\dots k_{j-1} \dots; \dots m'_j \dots]}{m_j^2 - m'^2_j} \\ = PV_{n+1}^X[\dots k_{j-1}, 0 \dots; \dots m_j, m'_j \dots], \quad (j \geq 2) , \end{aligned} \quad (\text{B.9})$$

with X being any set of Lorentz indices of momenta in the numerator of loop integrand.

For auxiliary scalar functions, defined in eqs. (B.4)–(B.6) this property manifests in a slightly more complicated manner. That is, depending on the position of m_j, m'_j within the brackets, the differences of \overline{PV}_n^i can either produce \overline{PV}_{n+1}^i or $\overline{PV}_{n+1}^{i+1}$. For the lowest order integrals, this property has the suggestive form

$$\frac{B_1[k_1, m_1, M_2] - B_1[k_1, m'_1, M_2]}{m_1^2 - m'^2_1} = C_{12}[0, k_1, m_1, m'_1, M_2] , \quad (\text{B.10})$$

$$\frac{B_1[k_1, M_1, m_2] - B_1[k_1, M_1, m'_2]}{m_2^2 - m'^2_2} = C_{11}[k_1, 0, M_1, m_2, m'_2] . \quad (\text{B.11})$$

For any order of scalar PV functions defined in (B.6) one has

$$\begin{aligned} \frac{\overline{PV}_n^i[\dots k_{j-1} \dots; \dots m_j \dots] - \overline{PV}_n^i[\dots k_{j-1} \dots; \dots m'_j \dots]}{m_j^2 - m'^2_j} \\ \stackrel{(j > i)}{=} \overline{PV}_{n+1}^i[\dots k_{j-1}, 0 \dots; \dots m_j, m'_j \dots] \\ \stackrel{(j \leq i)}{=} \overline{PV}_{n+1}^{i+1}[\dots k_{j-1}, 0 \dots; \dots m_j, m'_j \dots] . \end{aligned} \quad (\text{B.12})$$

Formulae (B.7)–(B.12) are particularly useful because their RHS's are explicitly regular in the limit of degenerate masses (as all functions defined by 1-loop integrals). Thus, they allow to generalise (3.6) to the case of mass matrices with degenerated diagonal elements.

References

- [1] **DONUT Collaboration** Collaboration, K. Kodama et al., *Observation of tau neutrino interactions*, *Phys.Lett.* **B504** (2001) 218–224, [[hep-ex/0012035](#)].
- [2] **D0** Collaboration, S. Abachi et al., *Observation of the top quark*, *Phys.Rev.Lett.* **74** (1995) 2632–2637, [[hep-ex/9503003](#)].
- [3] **CDF** Collaboration, F. Abe et al., *Observation of top quark production in $\bar{p}p$ collisions*, *Phys.Rev.Lett.* **74** (1995) 2626–2631, [[hep-ex/9503002](#)].
- [4] F. Englert and R. Brout, *Broken Symmetry and the Mass of Gauge Vector Mesons*, *Phys.Rev.Lett.* **13** (1964) 321–323.
- [5] P. W. Higgs, *Broken Symmetries and the Masses of Gauge Bosons*, *Phys.Rev.Lett.* **13** (1964) 508–509.
- [6] G. Guralnik, C. Hagen, and T. Kibble, *Global Conservation Laws and Massless Particles*, *Phys.Rev.Lett.* **13** (1964) 585–587.
- [7] **CMS** Collaboration, S. Chatrchyan et al., *Observation of a new boson at a mass of 125 GeV with the CMS experiment at the LHC*, *Phys.Lett.* **B716** (2012) 30–61, [[arXiv:1207.7235](#)].
- [8] **ATLAS** Collaboration, G. Aad et al., *Observation of a new particle in the search for the Standard Model Higgs boson with the ATLAS detector at the LHC*, *Phys.Lett.* **B716** (2012) 1–29, [[arXiv:1207.7214](#)].
- [9] S. Weinberg, *A Model of Leptons*, *Phys.Rev.Lett.* **19** (1967) 1264–1266.
- [10] G. Eilam, J. Hewett, and A. Soni, *Rare decays of the top quark in the standard and two Higgs doublet models*, *Phys.Rev.* **D44** (1991) 1473–1484.
- [11] B. Mele, S. Petrarca, and A. Soddu, *A New evaluation of the $t \rightarrow gt$; cH decay width in the standard model*, *Phys.Lett.* **B435** (1998) 401–406, [[hep-ph/9805498](#)].
- [12] S. Glashow, J. Iliopoulos, and L. Maiani, *Weak Interactions with Lepton-Hadron Symmetry*, *Phys.Rev.* **D2** (1970) 1285–1292.
- [13] H. P. Nilles, *Supersymmetry, Supergravity and Particle Physics*, *Phys.Rept.* **110** (1984) 1–162.
- [14] H. E. Haber and G. L. Kane, *The Search for Supersymmetry: Probing Physics Beyond the Standard Model*, *Phys.Rept.* **117** (1985) 75–263.
- [15] S. P. Martin, *A Supersymmetry primer*, *Adv.Ser.Direct.High Energy Phys.* **21** (2010) 1–153, [[hep-ph/9709356](#)].
- [16] J. Guasch and J. Sola, *FCNC top quark decays: A Door to SUSY physics in high luminosity colliders?*, *Nucl.Phys.* **B562** (1999) 3–28, [[hep-ph/9906268](#)].
- [17] J. Cao, G. Eilam, M. Frank, K. Hikasa, G. Liu, et al., *SUSY-induced FCNC top-quark processes at the large hadron collider*, *Phys.Rev.* **D75** (2007) 075021, [[hep-ph/0702264](#)].

- [18] J. Cao, G. Eilam, K.-i. Hikasa, and J. M. Yang, *Experimental constraints on stop-scharm flavor mixing and implications in top-quark FCNC processes*, *Phys.Rev.* **D74** (2006) 031701, [[hep-ph/0604163](#)].
- [19] J. Diaz-Cruz, H.-J. He, and C. Yuan, *Soft SUSY breaking, stop scharm mixing and Higgs signatures*, *Phys.Lett.* **B530** (2002) 179–187, [[hep-ph/0103178](#)].
- [20] J. Cao, C. Han, L. Wu, J. M. Yang, and M. Zhang, *SUSY induced top quark FCNC decay $t \rightarrow ch$ after Run I of LHC*, [arXiv:1404.1241](#).
- [21] **ATLAS Collaboration** Collaboration, G. Aad et al., *Search for top quark decays $t \rightarrow qH$ with $H \rightarrow \gamma\gamma$ using the ATLAS detector*, *JHEP* **1406** (2014) 008, [[arXiv:1403.6293](#)].
- [22] **CMS Collaboration**, CMS-PAS-HIG-13-034, *Combined $t \rightarrow cH$ limit from multi-lepton and di-photon analyses*, .
- [23] **Top Quark Working Group** Collaboration, K. Agashe et al., *Snowmass 2013 Top quark working group report*, [arXiv:1311.2028](#).
- [24] **ATLAS Collaboration**, ATLAS-CONF-2013-012, *Sensitivity of ATLAS at HL-LHC to flavour changing neutral currents in top quark decays $t \rightarrow cH$, with $H \rightarrow \gamma\gamma$* , .
- [25] J. Aguilar-Saavedra and G. Branco, *Probing top flavor changing neutral scalar couplings at the CERN LHC*, *Phys.Lett.* **B495** (2000) 347–356, [[hep-ph/0004190](#)].
- [26] C. Kao, H.-Y. Cheng, W.-S. Hou, and J. Sayre, *Top Decays with Flavor Changing Neutral Higgs Interactions at the LHC*, *Phys.Lett.* **B716** (2012) 225–230, [[arXiv:1112.1707](#)].
- [27] Y. Wang, F. P. Huang, C. S. Li, B. H. Li, D. Y. Shao, et al., *Constraints on flavor-changing neutral-current Htq couplings from the signal of tH associated production with QCD next-to-leading order accuracy at the LHC*, *Phys.Rev.* **D86** (2012) 094014, [[arXiv:1208.2902](#)].
- [28] N. Craig, J. A. Evans, R. Gray, M. Park, S. Somalwar, et al., *Searching for $t \rightarrow ch$ with Multi-Leptons*, *Phys.Rev.* **D86** (2012) 075002, [[arXiv:1207.6794](#)].
- [29] K.-F. Chen, W.-S. Hou, C. Kao, and M. Kohda, *When the Higgs meets the Top: Search for $t \rightarrow ch^0$ at the LHC*, [arXiv:1304.8037](#).
- [30] D. Atwood, S. K. Gupta, and A. Soni, *Constraining the flavor changing Higgs couplings to the top-quark at the LHC*, [arXiv:1305.2427](#).
- [31] M. Gorbahn and U. Haisch, *Searching for $t \rightarrow c(u)h$ with dipole moments*, [arXiv:1404.4873](#).
- [32] A. Greljo, J. F. Kamenik, and J. Kopp, *Disentangling Flavor Violation in the Top-Higgs Sector at the LHC*, [arXiv:1404.1278](#).
- [33] L. Wu, *Enhancing thj Production from Top-Higgs FCNC Couplings*, [arXiv:1407.6113](#).

- [34] L. Girardello and M. T. Grisaru, *Soft Breaking of Supersymmetry*, *Nucl.Phys.* **B194** (1982) 65.
- [35] L. Hall and L. Randall, *Weak scale effective supersymmetry*, *Phys.Rev.Lett.* **65** (1990) 2939–2942.
- [36] F. Borzumati, G. R. Farrar, N. Polonsky, and S. D. Thomas, *Soft Yukawa couplings in supersymmetric theories*, *Nucl.Phys.* **B555** (1999) 53–115, [[hep-ph/9902443](#)].
- [37] J. Hetherington, *The Spectrum of the MSSM with nonstandard supersymmetry breaking*, *JHEP* **0110** (2001) 024, [[hep-ph/0108206](#)].
- [38] G. D’Ambrosio, G. Giudice, G. Isidori, and A. Strumia, *Minimal flavor violation: An Effective field theory approach*, *Nucl.Phys.* **B645** (2002) 155–187, [[hep-ph/0207036](#)].
- [39] A. Dery, A. Efrati, Y. Nir, Y. Soreq, and V. Susic, *Model building for flavor changing Higgs couplings*, [arXiv:1408.1371](#).
- [40] F. Gabbiani, E. Gabrielli, A. Masiero, and L. Silvestrini, *A Complete analysis of FCNC and CP constraints in general SUSY extensions of the standard model*, *Nucl.Phys.* **B477** (1996) 321–352, [[hep-ph/9604387](#)].
- [41] M. Misiak, S. Pokorski, and J. Rosiek, *Supersymmetry and FCNC effects*, *Adv.Ser.Direct.High Energy Phys.* **15** (1998) 795–828, [[hep-ph/9703442](#)].
- [42] G. F. Giudice, M. Nardecchia, and A. Romanino, *Hierarchical Soft Terms and Flavor Physics*, *Nucl.Phys.* **B813** (2009) 156–173, [[arXiv:0812.3610](#)].
- [43] J. Rosiek, P. Chankowski, A. Dedes, S. Jager, and P. Tanedo, *SUSY_FLAVOR: A Computational Tool for FCNC and CP-Violating Processes in the MSSM*, *Comput.Phys.Commun.* **181** (2010) 2180–2205, [[arXiv:1003.4260](#)].
- [44] A. Crivellin, J. Rosiek, P. Chankowski, A. Dedes, S. Jaeger, et al., *SUSY_FLAVOR v2: A Computational tool for FCNC and CP-violating processes in the MSSM*, *Comput.Phys.Commun.* **184** (2013) 1004–1032, [[arXiv:1203.5023](#)].
- [45] J. Rosiek, *SUSY FLAVOR v2.5: a computational tool for FCNC and CP-violating processes in the MSSM*, [arXiv:1410.0606](#).
- [46] C. Zhang and F. Maltoni, *Top-quark decay into Higgs boson and a light quark at next-to-leading order in QCD*, *Phys.Rev.* **D88** (2013) 054005, [[arXiv:1305.7386](#)].
- [47] A. Czarnecki, J. G. Korner, and J. H. Piclum, *Helicity fractions of W bosons from top quark decays at NNLO in QCD*, *Phys.Rev.* **D81** (2010) 111503, [[arXiv:1005.2625](#)].
- [48] J. Rosiek, *Complete Set of Feynman Rules for the Minimal Supersymmetric Extension of the Standard Model*, *Phys.Rev.* **D41** (1990) 3464.
- [49] J. Rosiek, *Complete set of Feynman rules for the MSSM: Erratum*, [hep-ph/9511250](#).
- [50] A. Dedes, J. Rosiek, and P. Tanedo, *Complete One-Loop MSSM Predictions for $B \rightarrow ll'$ at the Tevatron and LHC*, *Phys.Rev.* **D79** (2009) 055006, [[arXiv:0812.4320](#)].

- [51] A. Crivellin, *Effective Higgs Vertices in the generic MSSM*, *Phys.Rev.* **D83** (2011) 056001, [[arXiv:1012.4840](#)].
- [52] A. Crivellin, L. Hofer, and J. Rosiek, *Complete resummation of chirally-enhanced loop-effects in the MSSM with non-minimal sources of flavor-violation*, *JHEP* **1107** (2011) 017, [[arXiv:1103.4272](#)].
- [53] J. F. Gunion, H. E. Haber, G. L. Kane, and S. Dawson, *The Higgs Hunter's Guide*, *Front.Phys.* **80** (2000) 1–448.
- [54] A. Djouadi, *Implications of the Higgs discovery for the MSSM*, *Eur.Phys.J.* **C74** (2014) 2704, [[arXiv:1311.0720](#)].
- [55] **ATLAS Collaboration**, ATLAS-CONF-2013-090, *Search for charged Higgs bosons in the τ +jets final state with pp collision data recorded at $\sqrt{s} = 8$ TeV with the ATLAS experiment*, .
- [56] M. Drees, *A Supersymmetric Explanation of the Excess of Higgs-Like Events at the LHC and at LEP*, *Phys.Rev.* **D86** (2012) 115018, [[arXiv:1210.6507](#)].
- [57] A. J. Buras, A. Romanino, and L. Silvestrini, *K to π neutrino anti-neutrino: A Model independent analysis and supersymmetry*, *Nucl.Phys.* **B520** (1998) 3–30, [[hep-ph/9712398](#)].
- [58] A. Dedes, M. Paraskevas, J. Rosiek, K. Suxho, and K. Tamvakis, *Mass Insertion vs. Mass Eigenstate calculations in Flavour Physics, work in progress*.
- [59] **Particle Data Group Collaboration**, J. Beringer et al., *Review of Particle Physics (RPP)*, *Phys.Rev.* **D86** (2012) 010001.
- [60] **ATLAS Collaboration** Collaboration, G. Aad et al., *Search for new phenomena in final states with large jet multiplicities and missing transverse momentum at $\sqrt{s} = 8$ TeV proton-proton collisions using the ATLAS experiment*, *JHEP* **1310** (2013) 130, [[arXiv:1308.1841](#)].
- [61] A. Delgado, G. F. Giudice, G. Isidori, M. Pierini, and A. Strumia, *The light stop window*, *Eur.Phys.J.* **C73** (2013) 2370, [[arXiv:1212.6847](#)].
- [62] M. R. Buckley, T. Plehn, and M. J. Ramsey-Musolf, *Stop on Top*, *Phys.Rev.* **D90** (2014) 014046, [[arXiv:1403.2726](#)].
- [63] C. Baker, D. Doyle, P. Geltenbort, K. Green, M. van der Grinten, et al., *An Improved experimental limit on the electric dipole moment of the neutron*, *Phys.Rev.Lett.* **97** (2006) 131801, [[hep-ex/0602020](#)].
- [64] S. Heinemeyer, W. Hollik, and G. Weiglein, *The Mass of the lightest MSSM Higgs boson: A Compact analytical expression at the two loop level*, *Phys.Lett.* **B455** (1999) 179–191, [[hep-ph/9903404](#)].
- [65] H. E. Haber, R. Hempfling, and A. H. Hoang, *Approximating the radiatively corrected Higgs mass in the minimal supersymmetric model*, *Z.Phys.* **C75** (1997) 539–554, [[hep-ph/9609331](#)].

- [66] J. Frere, D. Jones, and S. Raby, *Fermion Masses and Induction of the Weak Scale by Supergravity*, *Nucl.Phys.* **B222** (1983) 11.
- [67] C. Kounnas, A. Lahanas, D. V. Nanopoulos, and M. Quiros, *Low-Energy Behavior of Realistic Locally Supersymmetric Grand Unified Theories*, *Nucl.Phys.* **B236** (1984) 438.
- [68] J. Gunion, H. Haber, and M. Sher, *Charge/Color Breaking Minima and A-Parameter Bounds in Supersymmetric Models*, *Nucl.Phys.* **B306** (1988) 1.
- [69] J. Casas, A. Lleyda, and C. Munoz, *Strong constraints on the parameter space of the MSSM from charge and color breaking minima*, *Nucl.Phys.* **B471** (1996) 3–58, [[hep-ph/9507294](#)].
- [70] A. Riotto and E. Roulet, *Vacuum decay along supersymmetric flat directions*, *Phys.Lett.* **B377** (1996) 60–66, [[hep-ph/9512401](#)].
- [71] A. Kusenko, P. Langacker, and G. Segre, *Phase transitions and vacuum tunneling into charge and color breaking minima in the MSSM*, *Phys.Rev.* **D54** (1996) 5824–5834, [[hep-ph/9602414](#)].
- [72] J. Casas and S. Dimopoulos, *Stability bounds on flavor violating trilinear soft terms in the MSSM*, *Phys.Lett.* **B387** (1996) 107–112, [[hep-ph/9606237](#)].
- [73] C. Le Mouel, *Optimal charge and color breaking conditions in the MSSM*, *Nucl.Phys.* **B607** (2001) 38–76, [[hep-ph/0101351](#)].
- [74] J.-h. Park, *Metastability bounds on flavour-violating trilinear soft terms in the MSSM*, *Phys.Rev.* **D83** (2011) 055015, [[arXiv:1011.4939](#)].
- [75] J. Camargo-Molina, B. O’Leary, W. Porod, and F. Staub, *Stability of the CMSSM against sfermion VEVs*, *JHEP* **1312** (2013) 103, [[arXiv:1309.7212](#)].
- [76] N. Blinov and D. E. Morrissey, *Vacuum Stability and the MSSM Higgs Mass*, *JHEP* **1403** (2014) 106, [[arXiv:1310.4174](#)].
- [77] D. Chowdhury, R. M. Godbole, K. A. Mohan, and S. K. Vempati, *Charge and Color Breaking Constraints in MSSM after the Higgs Discovery at LHC*, *JHEP* **1402** (2014) 110, [[arXiv:1310.1932](#)].
- [78] W. Altmannshofer, C. Frugiuele, and R. Harnik, *Fermion Hierarchy from Sfermion Anarchy*, [arXiv:1409.2522](#).
- [79] J. Camargo-Molina, B. O’Leary, W. Porod, and F. Staub, **Vevacious: A Tool For Finding The Global Minima Of One-Loop Effective Potentials With Many Scalars**, *Eur.Phys.J.* **C73** (2013) 2588, [[arXiv:1307.1477](#)].
- [80] S. Pokorski, J. Rosiek, and C. A. Savoy, *Constraints on phases of supersymmetric flavor conserving couplings*, *Nucl.Phys.* **B570** (2000) 81–116, [[hep-ph/9906206](#)].
- [81] B. Allanach, C. Balazs, G. Belanger, M. Bernhardt, F. Boudjema, et al., *SUSY Les Houches Accord 2*, *Comput.Phys.Commun.* **180** (2009) 8–25, [[arXiv:0801.0045](#)].
- [82] A. Axelrod, *Flavor Changing Z^0 Decay and the Top Quark*, *Nucl.Phys.* **B209** (1982) 349.